FLOW ANALYSIS IN SCOUR HOLE AROUND BRIDGE PIER USING ANSYS FLUENT

A Dissertation submitted in partial fulfilment of the requirement for the
Award of degree of

MASTER OF TECHNOLOGY
IN
HYDRAULICS AND WATER RESOURCES ENGINEERING
BY

SAURABH KHANNA
(2K15/HFE/13)

Under The Guidance of

Dr. T. VIJAYA KUMAR

Associate Professor
Department of Civil Engineering
Delhi Technological University
Delhi

DELHI TECHNOLOGICAL UNIVERSITY
(FORMELY DELHI COLLEGE OF ENGINEERING)
DELHI-110042
JULY 2017

DELHI TECHNOLOGICAL UNIVERSITY
Established by Govt. Of Delhi vide Act 6 of 2009
(Formerly Delhi College of Engineering)
SHAHBAD DAULATPUR-110042

CERTIFICATE

This is to certify that the dissertation title "**Flow Analysis in Scour Hole Around Bridge Pier Using Ansys Fluent"** based on guidance in the academic session 2016-17. To the best of my belief "**Flow Analysis in Scour Hole Around Bridge Pier**" submitted by **Mr. SAURABH KHANNA, Roll. No. 2K15/HFE/13**, in partial fulfilment for the award of degree of Master of Technology in "**Hydraulics and Water Resources Engineering",** run by Department of Civil Engineering in Delhi Technological University during the year 2015-2017, is a bonafide record of student's own work carried out by him under my supervision.

Dr. T. VIJAYA KUMAR
Supervisor
Assistant Professor (CIVIL)
Delhi Technological University

CANDIDATES'S DECLARATION

I do hereby certify that the work presented is the report entitled **"FLOW ANALYSIS IN SCOUR HOLE AROUND BRIDGE USING ANSYS FLUENT**" in the partial fulfilment of the requirements for the award of the degree of "Master of Technology" in Hydraulics & Water Resources Engineering submitted in the Department of Civil Engineering, Delhi Technological University, is an authentic record of my own work carried out from January 2017 to July 2017 under the supervision of **Dr. T.VIJAYA KUMAR** (Associate Professor), Department of Civil engineering.

I have not submitted the matter embodied in the report for the award of any other degree or diploma.

Date: 31/07/2017

SAURABH KHANNA
2K15/HFE/13

ACKNOWLEDGEMENT

I take this opportunity to express my profound gratitude and deep regards to **Dr. T Vijaya Kumar** (Associate Professor, Civil Engineering Department, DTU) for his exemplary guidance, monitoring and constant encouragement throughout the course of this project work. The blessing, help and guidance given by him from time to time shall carry me a long way in life on which I am going to embark.

I would also like to thank Prof. Dr. Nirendra Dev (Head of Department, Civil Engineering Department, DTU) for extending his support and Guidance.

Professors and faculties of the department of Civil Engineering, DTU, have always extended their full co-operation and help. They have been kind enough to give their opinions on the project matter; I am deeply obliged to them. They have been a source of encouragement and have continuously been supporting me with their knowledge base, during study. Several of well wishers extended their help to me directly or indirectly and we grateful to all of them without whom it would have been impossible for me to carry on my work.

ABSTRACT

The flow pattern around a bridge pier is complex to understand and the complexity increases with the development of a scour hole. As a result of scouring in piers , collapse of peirs in bridges can easily occur so it is very important to understand the variation of flow in and around the piers to take some factor of safety in constructing piers. In this study our aim is to simulate the flow around pier and to determine parameters such as shear stress,scour depth and velocity profiles. Flow is being simulated using different models. The models include mesh free models and mesh based models.They are made using RANS model (Reynolds Averaged Navier Stokes and continuity equations. Models are made in 3D and fine meshing of the models is being done to make comprehensive study. Models are also being made using SPH(smoothed particle hydrodynamics)for mesh free models .The equations used in this type of modelling are Lagrangian eqautions known as Navier Stokes equations. Similar geometric and kinematic conditions were created in ANSYS as used in laboratory experiment. The common conclusion is that both models predict a downflow near the upstream nose of the pier which would affect the stability of pier foundations. Velocity profiles from mesh free models and mesh based models at different locations are compared. They also help in obtaining significant knowledge regarding scouring of sediment in pier and particle approximation.

Another new finding is the occurrence of flow separation and complex vortex stretching confined to the upper water column behind the pier. The predicted bed shear stress and turbulent kinetic energy are shown to compare well with the experimental data. Application of the mesh-free model to the flow in a scour hole around a bridge pier has been successful in generating desired approach flow. The results presented in this thesis are of practical values for prediction of sediment scour around bridge piers.

Table of Contents

LIST OF FIGURES

LIST OF TABLES

LIST OF SYMBOLS

B= Channel width on both sides of the pier (m)

D= Pier diameter (m)

C= Log-layer constant (N-m)

c= Speed of sound (m/s)

c_o= Reference speed of sound in water (m/s)

e= Internal energy (-)

F= Volume fraction (-)

F_a= Volume fraction of air (-)

F_w= Volume fraction of water (-)

F_r= Froude Number (-)

g= Acceleration of gravity (m/s^2)

h= Smoothing length (m)

h_o= Initial depth outside the scour hole (m)

k= Turbulent kinetic energy (m^2/s^2)

κ= Von karman constant (-)

L_1= Channel length upstream of the pier (m)

L_2= Channel length downstream of the pier (m)

N= Number of particles (-)

p= Instantaneous pressure component (N/m^2)

P= Reynolds-averaged pressure (N/m^2)

p'= Turbulent fluctuation component of pressure (N/m^2)

Pr= Turbulence production term (-)

Q= Discharge (m^3/s)

q= Discharge per unit width (m^2/s)

R_e= Reynolds Number (-)

S_{ij}= Mean flow strain rate (-)

t= Time (s)

W= Smoothing kernel function (-)

Δt= Time step (s)

u= Instantaneous velocity component in x direction (m/s)

U= Mean velocity component in x direction (m/s)

u'= Velocity fluctuation component in x direction (m/s)

u^+= Near wall velocity (m/s)

u_τ= Frictional velocity (m/s)

u^*= Shear velocity (m/s)

U_t= Velocity tangent to the wall (m/s)

Un_w= Velocity normal to the wall (m/s)

u_o= Depth averaged approach flow velocity (m/s)

v= Instantaneous velocity component in y direction (m/s)

V= Mean velocity component in y direction (m/s)

v'= Velocity fluctuation component in y direction (m/s)

w= Instantaneous velocity component in z direction (m/s)

W= Mean velocity component in z direction (m/s)

w'= Velocity fluctuation component in z direction (m/s)

y^+= Dimensionless distance from the wall (-)

Δy= Distance from the wall (m)

ε= Turbulent dissipation rate (m^2/s^3)

ρ_o= Reference water density (kg/m^3)

ρ_a= Density of air (kg/m^3)

ρ_w= Density of water (kg/m^3)

τ= Viscous stress (N/m^2)

τ_{ij}= Reynolds shear stress tensor (N/m^2)

τ_w= Wall shear stress (N/m^2)

σ= Total stress tensor (N/m^2)

μ= Dynamic viscosity of water (Ns/m^2)

ω= Energy dissipation per unit k (-)

ν_t= Turbulent eddy viscosity (m^2/s)

1 Chapter :Introduction

1.1 Background

Water flows in an open channel naturally along its path under the influence of gravity. In case of an obstacle in the flow, it changes its path .This can be compared to flow pattern around solid cylinder. As the flow is obstructed the flow changes direction in response to the obstacle. Such an instance can be the flow pattern in a channel with a cylinder inside the channel. As flow cannot proceed through the solid cylinder, it improvises its reaction bringing some changes in its path. This case resembles the flow in an open channel with a bridge pier.

Bridges are used to take roads and railways across the river. It rests on piers. The stability of bridge is proportional to that of piers. Change in path of flow results in change of bed level which leads to decrease in stability of pier. Modification in flow pattern around a pier results in channel-bed alteration and this phenomena is defined as local scour. The flow field around a pier is complex in detail and the complexity is aggravated with the development of scour hole. Scouring lowers the bed level around piers creating hole and threatens the stability of bridge foundations which yield bridge failures. It has been well-documented that" bridge pier scouring has been a significant transportation problem"(Shirole and Holt, 1991). A good understanding of the flow field is essential for safe pier-foundation design.

The complex process of scour development is poorly understood as evident from the literature survey presented in the next chapter. To improve our understanding, a more detailed description of the flow field must be obtained..Although there has been significant studies in the past regarding the problem of scouring flow but it is still very tough job to study the flow for the given conditions .The turbulent flow around a bridge has various scales of length and time so it is very complex and difficult to predict correctly. The flow characteristics are highly variable due to different types of piers and channel bed geometry .In case of 3D flow as in the case of turbulent flow where scouring takes place solutions are very complex to be produced.

In three-dimensional turbulent flow," the number of unknowns is more than the number of equations that can be established to solve for the unknowns (Wilcox, 1993)".In these cases experiments are not that economical. Numerical modelling is a good alternative approach.

Bridge piers with cylindrical shape (circular cross section) are the most general pier. As the flow goes around a pier, bed sediments from the flat bed geometry are often eroded. These eroded sediments again settle down slowly around the pier. The scouring rate is higher than the sediment settling rate at the beginning and at equilibrium both erosion and settling of sediments reaches a steady rate. The initially higher rate of scouring results in equilibrium fixed scour hole around a pier.

This numerical modelling research considers the bridge hydraulics problem where three-dimensional (3-D) open-channel flow approaches a fixed scour hole and interacts with a circular pier. The purpose of this research is to investigate the complex three-dimensional velocity field as a result of the interaction, which is difficult to measure in the laboratory and the field. The understanding of flow field around a pier is one of the most important aspects of bridge hydraulics. Flow approaching a bridge pier has tendency to move downward towards the channel bed which has implication in removing sediments from the channel bed. Excessive sediment removal or scouring is alarming for the safety of the bridge pier, which can eventually lead to uprooting of pier from the channel bed and yield bridge failure. So accuracy in the ability to predict local scouring around a bridge pier brings more confidence in safe pier-foundation design.

1.2 Objectives

The objectives of this thesis are:

- to predict the flow around pier of circular bridge using mesh based FEM method for detailed investigation of flow .
- to predict the flow around pier using SPH (smoothed particle hydrodynamics)in mesh free approach .
- to compare the results of both FEM and SPH with the experimental result

1.3 Scope of the work

To achieve the above-mentioned objectives, the rest of this thesis is organized as follows.

Chapter Two gives a summary of previous studies reported in the literature, on the topic of flow around bridge piers, including experimental and analytical studies on flow dynamics and the formation of turbulent eddies. Previous studies using different numerical solvers to resolve the flow field around piers with different pier shape and channel geometry will be reviewed. Progress made from the previous studies and outstanding issues will be discussed.

Chapter three, the model channel and setup of both the mesh-based FEM (CFX, ANSYS® Academic Research, Release 13.0) and mesh-free SPH simulations will be discussed. Details of boundary condition, initial condition, control parameter and their values (e.g. turbulence intensity, time stepping and kernel function) will be explained. Also, considerations of model domain dimensions for both FEM and SPH will be given.

Chapter four is devoted to presentation of the results from both FEM and SPH simulations. Analyses of the acquired data from the models will be further conducted. A direct comparison between the FEM model results and experimental results from Graf and Istiarto (2002) will be made.

Finally in **Chapter five**, the advantages and limitations of FEM and SPH in application to the bridge hydraulics problem will be discussed. Conclusions from the application will be drawn. Suggestions for future research on the topic of numerical modelling of scour-inducing flow around bridge piers will be made.

1.4 Contributions from the work

This research work has made significant contributions as described below:

- Finding out new tools for bridge hydraulic studies
- Generation of following data which helps in prediction of flow in scour hole
  Scour depth,Velocity profile, Vorticity profiles and Shear stress profile
- Helps to solve more difficult issues in case of bridge hydraulics.

2 Chapter : Literature Review

2.1 Bridge scour processes

"The local scour around bridge piers is one of the most common causes of bridge failures (Richardson and Davis, 2001)". "The fully three-dimensional flow around a cylindrical (circular in cross section) pier situated in a scour hole is schematically described in Figure 1(Richardson and Davis, 2001)." A pier is a support for a structure or superstructure such as arch or bridge .The flow when reaches the pier gets deflected in upward and downward direction .As soon as the flow reaches the pier at the upstream side bow wave is formed due to upward flow near the free surface .Bow wave is the progressive disturbance propagated through a fluid as a result of displacement by the foremost point moving through it at a speed greater than speed of wave across water .Due to the formation of the bow wave which is formed as a result of displacement at the foremost point of pier an acceleration in the flow takes place around the pier .There is a drawdown in the free surface due to this acceleration in the flow .The flow taking place in the center of the water column faces an obstacle so it has to pass around the pier .This separates the flow and the portion of it moves down along the upstream face of the pier .There is a difference in the pressure and velocity at the upstream and the downstream side of the pier due to which there is a pressure gradient and velocity gradient formation .Due to this pressure and velocity gradient flow interacts with the bed material which leads to the formation of horseshoe vortex at the base .The horseshoe vortex removes the material from the base as it has axis of rotation in horizontal direction ."These vortices with a horizontal axis of rotation remove bed material from the base at a greater rate of material transported to this region resulting in scour holes (Richardson and Davis, 2001). "With increasing scour depth, the horseshoe vortex loses its strength and live bed local scour turns into equilibrium scour (Richardson and Davis, 2001)". Live bed scour is the condition when the shear stress at the upstream face is greater than the threshold shear stress required to move the material from the bed .It means flow is getting continuously transporting sediments into a local scour hole .Live bed scour does not cause scour-

hole by itlsef .The reduction in the strength of horshoe vortex with increase in scour depth reduces shear stress at the upstream face and makes it smaller than the threshold shear stress which does not remove material at the upstream face so it does not fill the local scour hole which leads to the conversion of live scour into equilibrium scour. The equilibrium scour is the condition when the material transported by the approach flow is equal to the rate of local scouring .Wake vortices which have the vertical axis of rotation causes strong circulation and leads to the formation of wake region behind the pier .Both the type of vortex ,horseshoe vortex and wake vortex removes the material from the bed Critical issue is to analyse whether shear stress at the upstream part is less than or more than the threshold value needed to move the bed material .The maximum depth of scouring is achieved when the scour hole reduces the shear stress to the extent so that approaching flow can no longer remove bed material .This is called clear water condition .It occurs when shear stress at the upstream part is less than that of threshold value required to remove bed material .While analysing scour we should be able to differentiate between cohesive and non cohesive material .The non cohesive material is poorly researched and requires special attention .

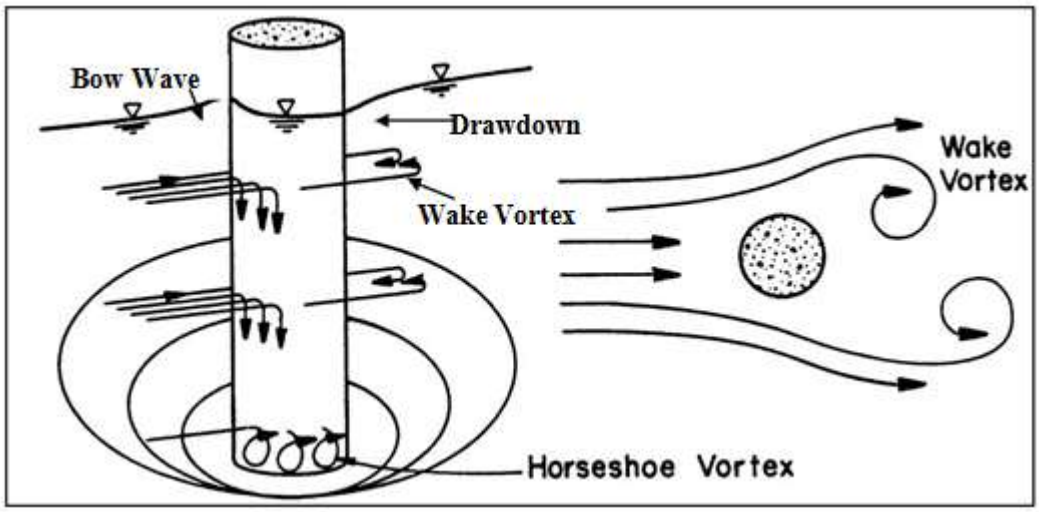

***Figure* 1** Schematic representation of flow around a circular pier (Richardson and Davis, 2001*).*

2.2 Experiments of bridge pier scour

Previously, investigators have made extensive laboratory measurements of flow velocity around piers, along with turbulence, bed shear stress and vortex shedding. Breuser*et al.* (1977) and Richardson *et al.* (1993) addressed the complexity in analysis of local scour at bridge pier as it requires various formulas that involve descriptions of mean flow field. Their application to complex flow patterns is problematic and often leads to questionable results in field applications, according to Landers and Mueller (1996). Laboratory and field investigations are time consuming and expensive. Due to recent advances, numerical solutions are increasingly considered to be a more reliable approach (Dargahi, 1987).

Melville (1974) conducted extensive measurements of the flow field, turbulence, bed shear stress and vortex shedding in the small-scale laboratory experiments with circular piers for rigid flat bed, intermediate scour hole and equilibrium bed. Dargahi (1987) presented detailed measurements for velocity, pressure, horseshoe vortex and bed shear stress. Yanmaz and Altinbilek (1991) performed sets of experiments using single cylindrical and square bridge pier models in the laboratory under clear water conditions with uniform bed materials. Semi empirical time-dependent analysis of local scour depths around bridge piers has been conducted using the sediment continuity equation for the scour hole around bridge piers. For design purposes, non-dimensional scour prediction curves were prepared in terms of various sediment and flow properties. Ahmed (1994) and Ahmed and Rajaratnam (1998) performed detailed measurement of flow field and turbulent boundary layer in front of circular piers. Sarker (1998) conducted extensive laboratory experiments for the flow field in front and behind of small-scale circular piers using the acoustic Doppler velocimeter. Beheshti and Ataie-Ashtiani (2010) experimentally investigated three-dimensional turbulent flow field around a complex bridge pier placed on a rough fixed bed. The complex pier foundation consisted of a column, a pile cap, and a 2x3 pile group where all the elements were exposed to the approaching flow. An acoustic Doppler velocimeter was used to measure instantaneously the three components of the velocities at different horizontal and vertical planes. Graf and Istiarto (2002) conducted experiment of the three-dimensional flow field in an established (equilibrium) scour hole and vorticity was calculated based on the measured instantaneous velocity components.

All the investigations have contributed to an improved understanding of the intricate scour process. They have also produced some useful empirical methods mainly for determining the maximum depth of scour, which is indeed of practical importance to the safe and cost-effective design of bridge piers. However, experimental investigations have an inherent limitation – that is the use of typically small-scale laboratory flumes. There are uncertainties in terms of artificial boundary effects and scaling; either Reynolds number or Froude number similarity has to be ignored due to difficulties in meeting both similarity laws.

2.3 Three-dimensional modelling of bridge pier scour

Mendoza-Cabrales (1993) used the standard k-ε turbulence model to solve three-dimensional flow in the vicinity of vertical circular piers and computed the associated bed shear stress but a large discrepancy was found compared to the experimental data of Melville (1974). Olsen and Malaaen (1993) used a steady state Navier-Stokes solver coupled with a sediment transport algorithm to simulate the growth of scour hole at the base of a circular pier. Ali et al. (1997) showed that the renormalization group (RNG) k-ε model gives a good estimation of the velocity field and bed shear stress. Dey et al. (1994) developed a three-dimensional semi-empirical kinematic model for vortex flow around circular piers in a quasi-equilibrium scour hole in a clear water regime. The velocity distribution pattern obtained by Melville (1974) matched satisfactorily with the model output results. Dou et al. (1998) calculated the anisotropic turbulence stresses and the associated bed shear stresses using the turbulence Reynolds stress model developed by Dou (1980).

Richardson et al. (1998) used a CFD model called FLOW-3D developed by Sicilian et al. (1987). The FLOW-3D model solves three-dimensional transient Navier-Stokes equations by the volume-of-fluid method developed by Hirt and Nicholas (1981). The model supported turbulent closure through a number of schemes including Prandtl's mixing length theory, the eddy viscosity model, the two equation k-ε model and the renormalized group (RNG) theory. The model output resulted infavorable qualitative and quantitative comparisons with experimental results by Melville and Raudkivi (1977).

Salaheldin et al. (2003) examined the performance of several turbulence models in simulating three-dimensional separated vertical flow field around circular piers utilizing a CFD solver FLUENT (FLUENT, 1998). Several variants of k-ε model and Reynolds stress model (RSM) has been used for turbulence closure. The computed velocity field and bed shear stress have been compared with some of experimental data available in literature like Melville (1974), Dargahi (1987) and Ahmed and Rajaratnam (1998). It appears that the standard and the RNG k-ε models are adequate for simulating the flow field around piers, but overestimate the near bed velocity. Reportedly, the Reynolds stress model gives the most acceptable results of velocity, bottom shear stress and water level in the case of flat bottom, and of velocity and water level in the case of equilibrium scour.

Huang et al. (2008) conducted numerical simulations to investigate the scale effect on turbulence flow and sediment scour near cylindrical bridge pier using FLUENT (ANSYS, 2007). Effect of scale on turbulence flow and sediment scour had been investigated by comparing different results obtained from full scale numerical model to those derived from Froude similarity method. In physical modeling either Reynolds or Froude similarity has to be ignored due to difficulty in meeting both similarity laws. But in this study using three-dimensional CFD model, both Froude and Reynolds number effects had been included. Though obtaining perfect results had been difficult due to many factors involved, Huang et al. concluded that the predicted flow patterns around the pier using FLUENT had exhibited good qualitative results.

Kirkil et al. (2008) conducted a study applying Large Eddy Simulation (LES) modeling aided by a laboratory experiment that aimed at delineating the coherent turbulence structures and their interactions in a scour hole formed at a circular cylinder founded in an alluvial bed at a relatively low Reynolds number for which Clearwater scour conditions persisted. The study report concluded that, the structure of the horseshoe vortex system was found to be more complex than previously indicated in scour literature. The numerically derived distribution of time-averaged bed-friction velocity around the cylinder had been found to concur with the equilibrium scour-hole bathymetry measured during the laboratory experiment.

2.4 Hydrodynamic applications of the SPH model

Monaghan (1992) applied the SPH (smoothed particle hydrodynamics) method for free surface particles incompressible flows phenomena such as dam-break, bore, wave maker and propagation of waves towards a beach. He found that the SPH method can simulate free surface flow without problems when given that the density is calculated approximating its rate of change and move with corrected velocity. SPH being an explicit numerical method, Monaghan concluded that use of an artificial equation of state makes the time step shorter than desirable.

Randles and Libersky (1996) made improvements and changes in SPH for both fluids and solids. The use of kernel renormalization and conservative smoothing method, the instability and poor accuracy issues of SPH method have been improved. The study concluded that fluid-structure interaction model being more robust and incorporating the void treatment for multiphase flow, has made the SPH method simpler to apply.

Gomez-Gesteira and Dalrymple (2003) modeled the impact of a single wave generated by a dam break with a tall structure using three-dimensional SPH model. Both the effects of having dry and wet bed in front of dam prior to dam break have been discussed in this study. The velocity field at a given position and force exerted by the wave on the structure have been successfully reproduced. The simulated velocity fields have also compared well with experimental results.

Shao (2004) simulated non-linear and dispersive solitary wave reflection and transmission characteristics after interacting with partially immersed curtain-type breakwater using the SPH method. The model easily tracked free surfaces by Lagrangian particles without numerical diffusion. Partially immersed curtain breakwaters have been found effective in dissipating incoming wave energy when the immersion depth was over half of the water depth. The wave force on the curtain wall reached only one single peak value in case of smaller waves and double peak value in case of larger non-linear waves.

Dalrymple and Rogers (2006) examined the propagation of highly nonlinear and breaking waves with the improved SPH tool implementing a different time stepping algorithm. The improvements made the SPH method to easily take care of turbulence, fluid viscosity and density. The method has performed very well for relatively small regions with lower number of particles. It was also concluded that the SPH method may not be suitable for larger number of particles.

Silvester and Cleary (2006) performed a three-dimensional dam-break flow and its interaction with a rectangular column downstream using the SPH model varying different simulation parameters. The results compared well with the existing experimental data. Crespo*et al.* (2007) studied the mitigation of force and moment exerted on structures by dikes with the three-dimensional SPH model. Interaction between both the water overtopping and flowing around the dike were found to be responsible for the force on the structure. The study concluded that the Lagrangian nature of SPH method permits the flow discontinuities without constraints due to presence of a grid.

Crespo*et al.* (2008) further analyzed the dam break evolution over dry and wet beds. The measured velocities from the two-dimensional SPH model reproduced the experimental dam break profiles accurately. It was found that although breaking dominates over wet beds in the beginning of movement, bottom friction turns into the principal dissipation mechanism later on. Staroszczyk (2010) simulated the two-dimensional dam break problem applying a SPH method with corrected smoothing kernel functions. The results from this exhibited better quantitative predictions of the wave front, with respect to time, than the standard SPH method.

Gomez-Gesteira*et al.* (2010) described the state-of-art of the classical SPH formulation of free surface flow phenomena such as two-dimensional and three-dimensional dam-break situations. Use of density filters and kernel correction for theimprovement of classic SPH approach has been performed. The study concluded that achieving higher accuracy depends on high number of particles with very small time steps. They suggested that combining SPH with other techniques to form hybrid

methods that might speed up computation. Groenenboom and Cartwright (2010) applied coupling of SPH and Finite Elements (FE) to fluid-structure interaction for the case of dam break in a container and drop of flexible cylinder in water. The robustness and versatility of the physics-based SPH-FE fluid-structure interaction results have demonstrated the maturity of the hybridized solver over stand-alone SPH solver.

Takbiri*et al.* (2010) analysed the seepage through dam foundation using SPH method. Comparison of seepage maps and results obtained from both SPH and FE methods were performed in this study. Chang *et al.* (2011) described application of a numerical mesh-free method which solved the shallow water equations based on SPH technique for dam-break flow simulation in one-dimensional open channels. Proposed methods have been validated conducting different problems. The models had produced accurate solutions that compared well with experimental and field data.

Hopton (2010) attempted to convert Hydra, the pre-existing SPH code for astrophysical simulations to simulate water flow phenomena such as dam bursting and flow over a weir. The study concluded that SPH method and Hydra accurately reproduced the flow characteristics of dam break problem. With increasing complexity in boundaries, the commercial package ANSYS CFX had achieved better solution than Hydra.

Vacondio*et al.* (2012) simulated flood inundation using a SPH model for shallow water equations (SWEs) implementing the open boundary conditions for the first time. The results have been found in good agreement with the results of commercial software TUFLOW and a finite volume scheme. The study concluded that the SPH-SWE numerical model can be successfully applied to flooding over initially dry and complex bathymetries.

Edge *et al.* (2012) applied SPH on Nvidia CUDA-enabled graphics card (GPUSPH) for modeling wave runup and overtopping applications. The best part of this method has been that GPUSPH allows the incorporation of very irregular bathymetry. The model results had shown good comparison with other numerical and experimental results. The study concluded that GPUSPH did not require much time for this simulation and this simulation time lowered with increasing cores in Nvidia graphics cards.

3 Chapter : Model Setup

3.1 Model channel and setup of FEM simulations

The model channel considered in the research is illustrated in Figure 3.1 in the Cartesian coordinates (x, y, z). The pier has a diameter of D = 14 cm. The red line symbols the stability position of the free water surface. Above this surface, there is a layer of air 0.66D thick. The fixed scour hole around the pier has the same bottom profile along the channel centerline as Graf and Istiarto's (2002) experimental channel. The model channel has a width of 8.40D on both sides of pier, and a length of 8D and 16.33D, respectively, upstream and downstream of the pier. The equilibrium water depth outside the scour hole is h_o = 2.4D. Water flow line of attack the scour hole from the positive direction of the *x*-axis or from left to right.

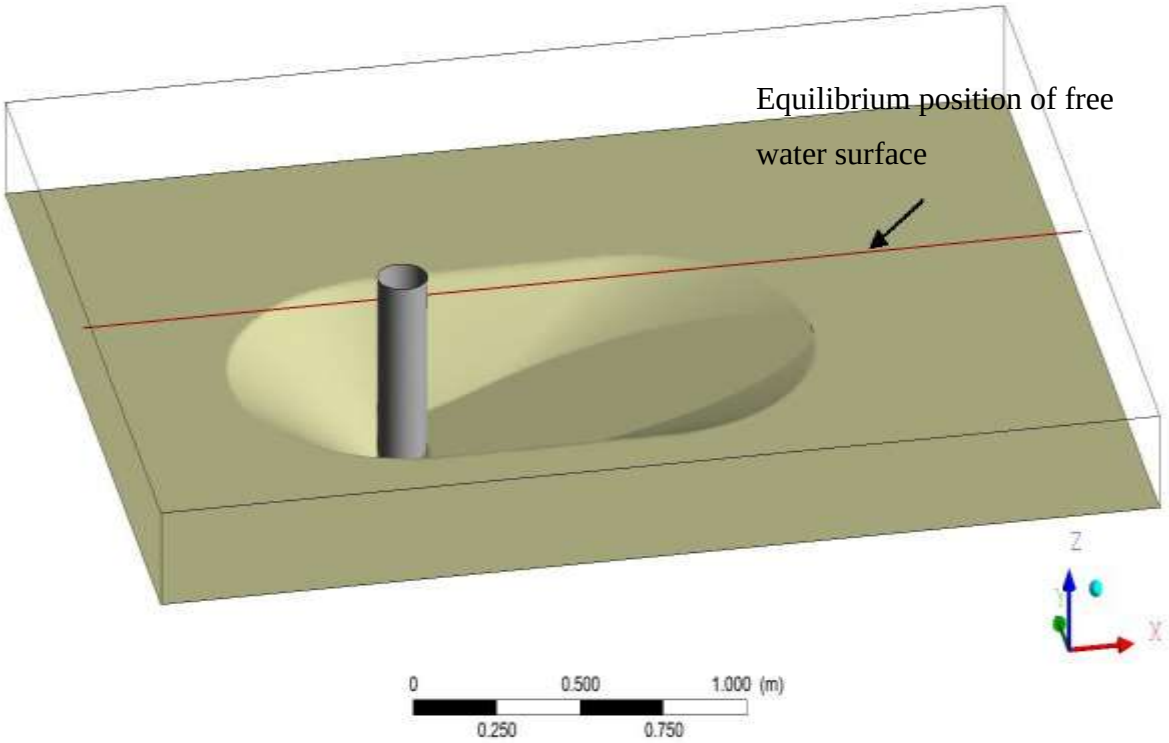

Figure 2 A three-dimensional view of the model channel used in mesh-based FEM simulations

Parameter/variable	Value	Unit
Time step	0.01	s
Simulation duration	15	s
Pier diameter		m
Channel length upstream of the pier	0.15	m
Channel length downstream of the pier	0.975	m
Channel width on both sides of the pier	2.075	m
Discharge	0.2	$\frac{m^3}{s}$
Initial water depth outside the scour hole	0.18	m
Initial thickness of air layer	0.05	m
Inclination of scour hole upstream of the pier	29	deg
Inclination of scour hole downstream of the pier	10	deg
Scour hole length upstream and downstream of pier	0.45,1.2	m

Table 3.1 : A summary of control parameter used in FEM simulations

The hydraulic conditions and channel geometry used in FEM simulations(Table 3.1) match the experiment setup of Graf and Istiarto (2002). This allows a direct comparison between the results from this modelling research and thelaboratory measurements of Graf and Istiarto (2002). A comparison will be made ofvertical profiles of predicted longitudinal velocity with available measured velocity profiles at 13 locations, labelled as f1 to f7 and b1 to b7 . In addition, acomparison of predicted and measured bed shear stresses distributed along the channel centreline will be presented. The approach flow has a depth-averaged velocity of u_o = 0.34 m/s. The Froude number is calculated to be 0.33, based on h_o andu_o. A two-phase flow problem was considered, where air at 24^{o}c and water are defined as model fluids, each being treated as a homogeneous continuous fluid. The interface between airand water or the free-water surface is specified as that the fluid particles on thesurface remain there all the time. There is no mass transfer across the interface. Reference pressure is set at 1 atm with gravity

acting in the negative z-direction.Heat transfer is fixed as isothermal at 24^{o}C temperature with air density of 2.184kg/m^{3}. The Reynolds number based on the approach flow is 91000.

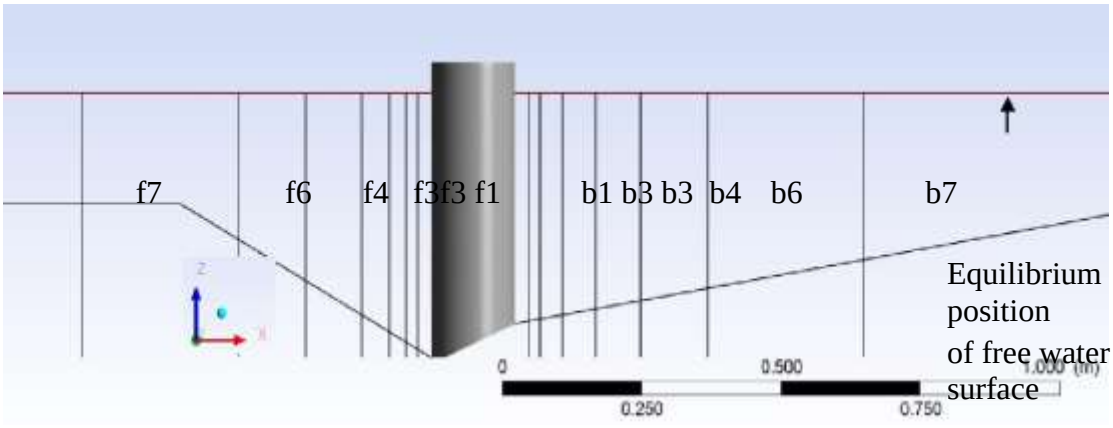

Figure 3 The vertical cross section through the model channel centreline, showing the bed-surface profile and 13 locations (f1 to f7 upstrem of the pier and b1 to b7 downstream) from which laboratory measurments of flow velocity (Graf and Istiarto, 2002)

3.2 Model channel in SPH simulations

The model domain used in mesh-free SPH simulations consists of an upstream headwater reservoir, a main channel that is similar to that used in the mesh-based FEM simulations, a channel extension downstream of the main channel and a downstream basin. This upstream reservoir has a height of 9 m, a length of 9 m and a width matching that of the main channel. The effects of dimensions chosen for the reservoir on the flow in the channel will be discussed in Chapter Three. A vertical gate, which can be lift in the vertical by up to 0.3 m, is placed between the upstream reservoir and the main channel. This gate controls water flow from the reservoir through the main channel to the downstream basin.

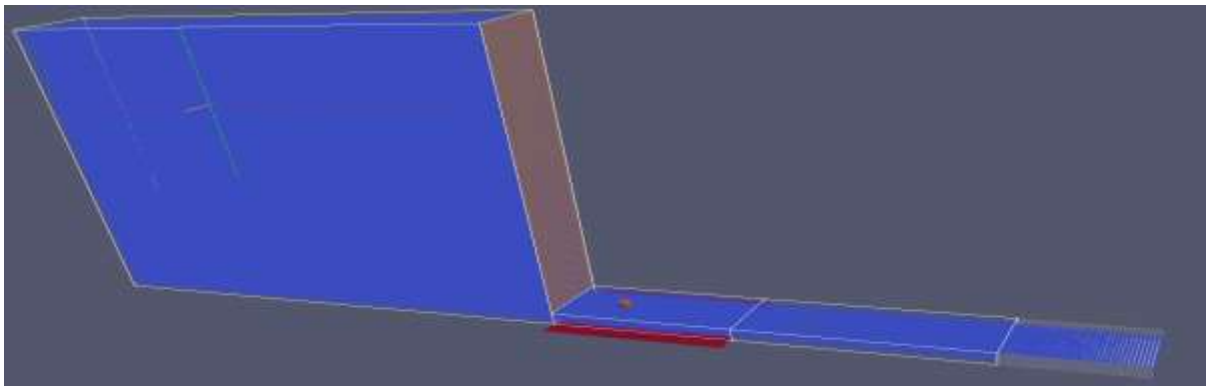

Figure 4 A three-dimensinal view of the model domain used in SPH simulations, showing a headwater reservoir, a main channel , an auxiliary channel extension downstream of the main channel and a downstream reservoir.

The main channel contains a fixed scour hole whose shape and size are the same as Graf and Istiarto's (2002) laboratory channel, although its width is made smaller than that of the laboratory channel. The width is reduced from 7.67D in the laboratory model to 4D in the SPH model on both sides of the pier. This is to reduce the total fluid volume in the main channel and hence lower the total number of particles needed to adequately represent the fluid volume. Through a series of sensitivity simulations, the effects of width reduction on SPH solutions will be analysed later in Chapter Four. The sensitivity simulations help finalise the main channel, being 3.04 m long and 1.67 m wide, with a scour hole and pier symmetric.

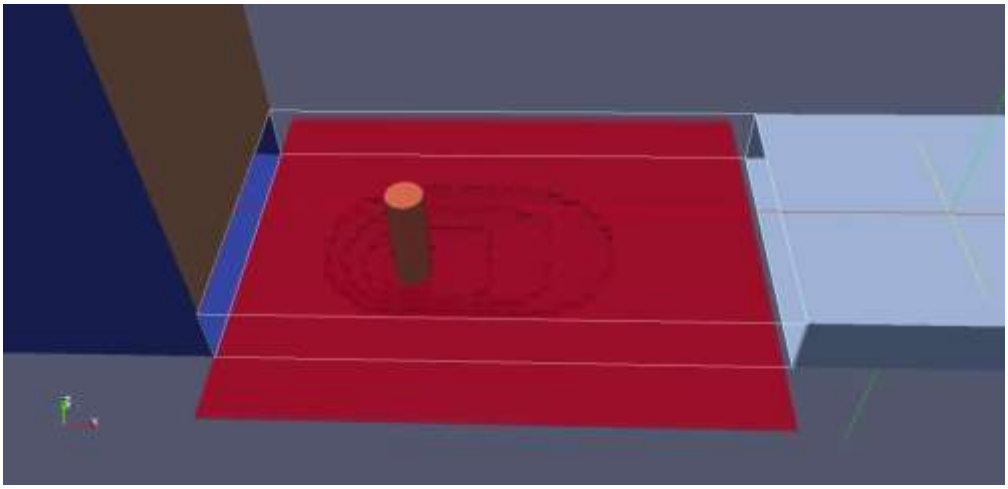

Figure 5 Close-up of the main channel showing details of the scour

In the process of setting up SPH simulations, the initial condition of a dry main channel was considered. In other words, the fluid exits the reservoir like a dam break and enters the main channel as free-surface flow . Without a lid over the water surface, it was difficult to control the water level in the main channel and to achieve the target flow depth of 0.18 m as in Graf & Istiarto's (2002) experiment. An adjustment of the fluid volume in the reservoir was found to help achieve the target flow depth, but was not able to produce, at the same time, an inflow velocity below the gate (or approach flow velocity) matching the experimental value of 0.34 m/s. In order to match the experimental values for approach flow depth as well as velocity, the water level was adjusted in the reservoir and introduced a horizontal lid on the top of the main channel. Test simulations with a lid on the top of the main channel produced vertical profiles of longitudinal velocity, which resemble closed-conduit flow rather than open-channel flow. The main feature is that the longitudinal velocity, U, increases with height, z,

from the channel-bed, reaches a peak value at a certain height and decreases further up toward the lid. To deal with this issue, a lid was placed at a height of 0.3 m. The idea is to produce a flow depth of 0.18 m between the channel-bed and the peak velocity height, and at the same time, this portion of the flow has the target depth-averaged velocity of 0.34 m/s. This treatment is acceptable for two simple reasons. First, the shear stress is zero at the peak velocity height, which dynamically resembles open-channel flow. Second, the free-water surface is not far from horizontal over the short length of the main channel. The use of 0.3 m, instead of 0.36 m (corresponding to an exact symmetry of 0.18 m for flow depth), is due to the loss of a thin layer of flow or streamlines near a solid boundary in SPH simulations.

Parameter/variable	**Value**	**Unit**
Time step	0.03	s
Pier diameter	0.15	m
Reservoir length,width,and height	9.0,1.65,9.0	m
Main channel length upstream of the pier	0.975	m
Main channel length downstream of the pier	2.075	m
Main channel width on both sides of the pier	0.825	m
Vertical opening of reservoir gate	0.40	m
Inclination of scour hole upstream of the pier	29	deg
Inclination of scour hole downstream of the pier	10	deg
Scour length upstream of the pier	0.45	m
Scour length downstream of the pier	1.2	m
Viscosity value	0.25	
Viscosity formulation	artificial	
Time step algorithm	Verlet	
Verlet steps	40	
Kernel section	Cubic spline	

Table 3.2 : A summary of control parameter used in SPH simulations

3.3 Time stepping in SPH simulations

The appropriate time duration for SPH simulations is estimated as follows: Initially, when water exits the upstream reservoir , the flow below the gate has a velocity of 0.34 m/s. Between the gate and the downstream end of the main channel, the horizontal distance is 3.04 m. Thus, flowing fluid particles will take 6.78 s to cover the distance. This value may be used as a reference value for the time duration to reach a steady state. The number of time steps corresponding to the time duration may be determined by dividing the duration by a chosen time step, Δt, for simulations.

Simulations use 6.27s as the model time duration or last 209 time steps with a time step of 0.03 s. As will be illustrated later in Chapter Four, the flow reaches a steady state after 100 time steps (or 3 s of model time) and therefore, the use of a total of more than 200 time steps is adequate to produce steady state flow field. The chosen time step of 0.03 s is small enough to avoid possible numerical noise or fluctuations in numerical solution from one time step to the next. A time series will be extracted of flow velocity at a number of selected locations from SPH results and examine them with respect to equilibrium and noise.

To maintain the approach flow at the desired velocity of 0.34 m/s over the entire simulation duration with a time step of 0.03 s, it is preferred to have a very small distance between fluid particles (*dx*, *dy* and *dz*) in the so-called numerical upstream reservoir and main channel. However, a decrease in the distance will lead to an increase in the total number of particles needed to fill up the numerical reservoir and channel. To optimise between the requirement and computational costs, the distance between fluid particles was chosen to be $dx = dy = dz = 0.03$ m.

4 Chapter : Results

4.1 The FEM Model

4.1.1 Sensitivity test and equilibrium solution

For the hydraulic conditions and channel geometry given in Table 3.1, a series of test simulations were carried out to test the independence of numerical solutions to the model equation on mesh configuration in terms of spatial resolution, mesh type and mesh inflation near a solid surface. The basic idea is to progressively refine the mesh on which simulations are performed until the simulated flow field is no longer sensitive to further refinement. The results from different test simulations have been compared quantitatively. When making mesh refinement, a special attention was paid to the scour hole region around the pier as this region is the focus of the present modelling research.

Table 4.1 Quantitative Comparison of flow velocities with different mesh resolutions.

Location	Velocity Components	R1	R2	R3
(0.2,0.4,0.1)	u	0.42	0.4	0.41
	v	0.013	-0.01	-0.01
	w	-0.033	-0.09	-0.094
(0.7,1.0,-0.04)	u	0.36	0.33	0.33
	v	0.007	-0.03	-0.01
	w	-0.104	-0.09	-0.093
(1.2,1.4,0.04)	u	0.33	0.3	0.32
	v	-0.021	-0.01	-0.039
	w	-0.003	-0.0009	0.002
(2.4,2.0,0.14)	u	0.33	0.3	0.33
	v	-0.003	-0.03	-0.02
	w	0.003	0.099	0.032

As an example of quantitative comparison, the predicted flow velocities (in m/s) at four locations: (x, y, z) = (0.2, 0.4, 0.1), (0.7, 1.0, -0.04), (1.2, 1.4, 0.04) and (2.4, 2.0, 0.14), for three simulations (R1, R2 and R3) with different mesh resolutions are shown in Table 3.1. Clearly, all the simulations produce consistent results.All the test simulations commence from a state of rest or from velocity (U, V,W) (0, 0, 0) everywhere in the model domain; the unsteady model equations are integrated over time for a prescribed time duration (14 second, see Table 3.1). The time duration is chosen to be sufficiently long to ensure that the numerical solution to the model equations reaches a state of equilibrium. The time duration was determined that was needed to reach an equilibrium as follows: First, estimate the advection time as the ratio of the total length of the model channel (L_1 + L_2 = 3.04 m, Table 3.1) to the average flow velocity in the approach channel (0.34 m/s). Then, multiply the advection time by a factor of 2.4 to obtain the simulation time duration (= 14 s, Table 3.1).An examination of the results (not shown) of equilibrium flow velocity and water surface elevation for the test simulations lead to the ultimate choice of a mesh system for use in subsequent simulations. The use of different mesh types, including tetrahedron, prism, pyramid and hexahedron, was found to have little influence on the results. A tetrahedron-type mesh was used in subsequent simulations. Mesh inflation at solid boundaries (such as the channel-bed and pier surface) is applied in order to effectively resolve near-boundary flow. The use of a mesh system with inflation has produced more realistic flow features.In FEM, mesh adaptation is available. This is a built-in feature in which the mesh in selected areas is refined with specified control criteria. The purpose of this feature is to accelerate solution convergence at any time step during a simulation, which must not be confused with the idea of testing the independence of solutions to mesh configuration. The mesh can be automatically adjusted at a selected time of simulation at locations where a defined solution variable is varying rapidly. Refining mesh at those points help resolve the flow features better. Mesh adaptation for different solution variables were tested. Applying mesh adaptation after 100 iterations for solutions of the volume of fraction of water was selected. It is appropriate for the multiphase flow simulation performed in our case based on the test simulations.

4.1.2 Velocity vector field in the horizontal

Velocity vectors at a depth of 0.09 m or 0.6D below the free surface are plotted. Upstream of the pier, water flows around the pier. The presence of the pier in the flow path results in velocity vectors different from location to location in both magnitude and direction, and gives rise to strong clockwise and counter-clockwise circulations just downstream of the pier or wake vortices. Flow separation from the pier surface is visible. At 0.09 m below the free water surface the longitudinal or x-component of velocity ranges from -0.33 to 0.63 m/s (compared to the approach flow velocity of u_o = 0.34 m/s). The negative values are associated with wake vortices. The transverse or y-component of flow velocity ranges from -0.26 to 0.32 m/s. The influence of the pier on the flow field diminishes far downstream, where velocity vectors regain uniformity (not shown).

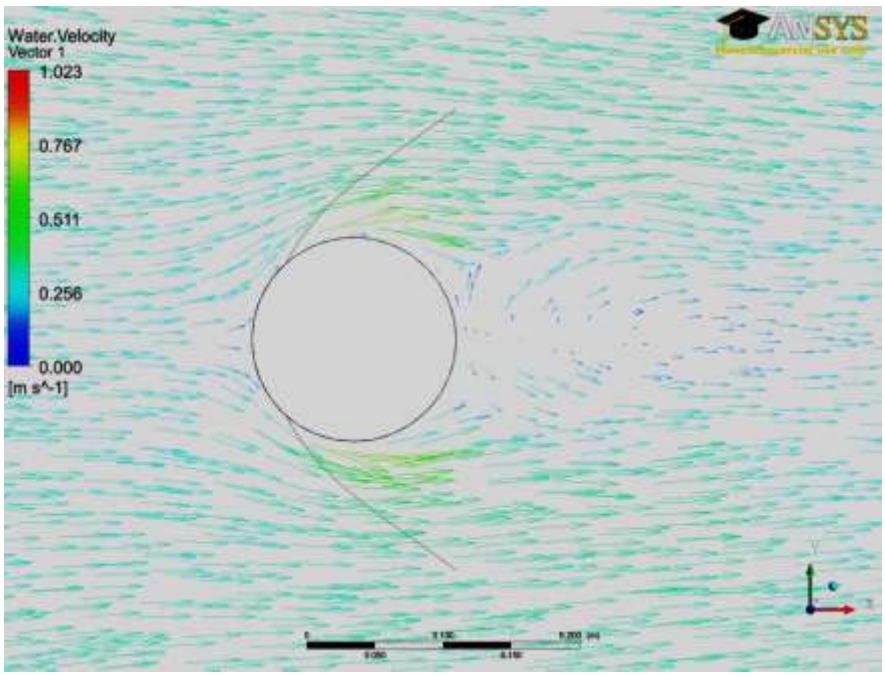

Figure 6 A horizontal plane showing velocity vectors at a depth of 0.09 m below the free surface

Velocity vectors in the scour hole at about half the maximum scour depth are shown in Figure 7. The flow shows divergent patterns near the upstream edge of the scour hole. Associated with the divergence is an upward flow from below (not shown). No flow separation is visible. Presumably, this is because the flow accelerates under the influence of the rising channel-bed downstream of the pier, which creates a favourable pressure gradient. At 0.34 m below the free water surface the longitudinal and transverse (or x and y) components of flow velocity range from -0.13 to 0.43 m/s and from -0.26 to 0.32 m/s, respectively. As expected,as the flow depth increases the flow velocities inside the scour hole have smaller magnitudes than those above the scour hole .

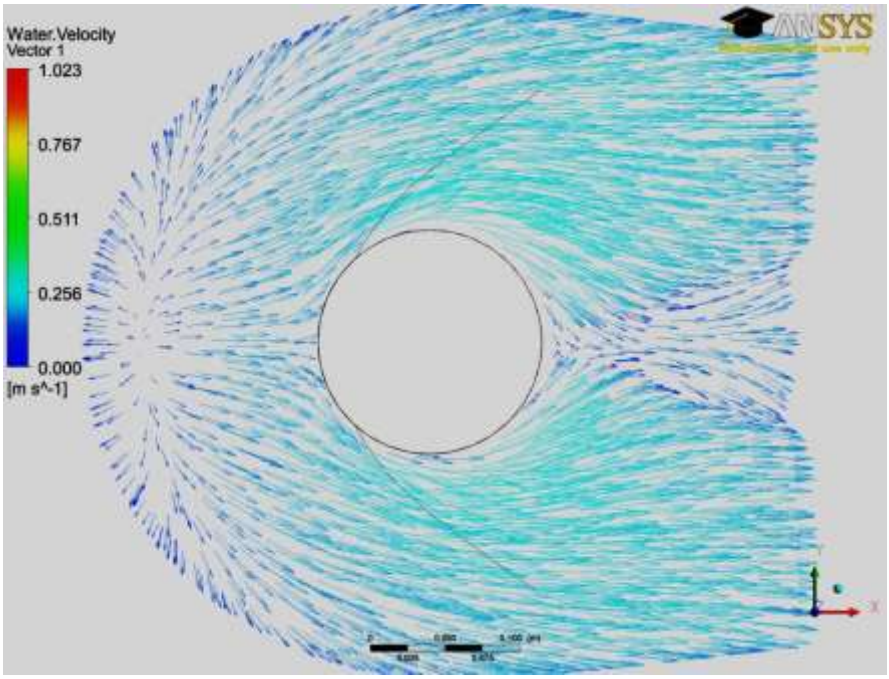

Figure 7 A horizontal plane showing velocity vectors inside the scour hole at a depth of 0.34 m below the water surface.

4.1.3 Flow streamlines

Vortex motions around the pier are clearly shown as streamlines in Figure 9. A number of observations can be made: (a) the streamlines wrap around the upstream half of the pier at all depths between the free surface and the channel-bed; (b) the streamlines wrap around the entire pier surface over the lower half of the pier, where there is no significant flow separation; (c) from the free surface down to about one third of the pier diameter and downstream of the pier, the streamlines detach from the

pier surface, meaning that flow separation takes place there; (d) at a short distance (0.37 to 0.8D) below the free surface, vortex stretching occurs. The implications are that it would be extremely difficult to measure the complex flow features and vortex motions in laboratory experiments.

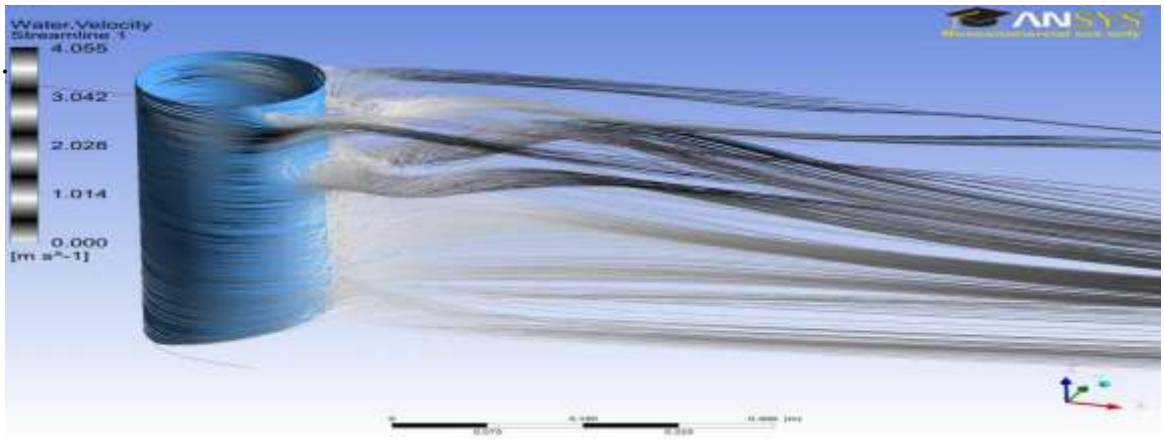

Figure 7 Streamlines around the pier, showing flow separation downstream of the pier near free surface and vortex stretching at a short distance below free surface.

4.1.4 Velocity structures in the vertical direction

As illustrated in Figure 10, the flow field in the scour hole region is very elaborate. Water enters the scour hole as a jet hugging the bed, with a core of high speed ($\approx 1.4u_{o,}$ where u_o is the approach flow velocity equal to 0.34 m/s). Further into the scour hole, eddy motions are visible immediately above the sloping bed. Close to the pier, water flow is deflected downward. Both the eddy motions and downward flow have important implications for the movement of bed sediments. Downstream of the pier, the flow is weak, compared to the condition upstream of the pier, but the flow patterns are much more complicated. This is particularly the case immediately downstream of the pier; the flow is mainly upward.

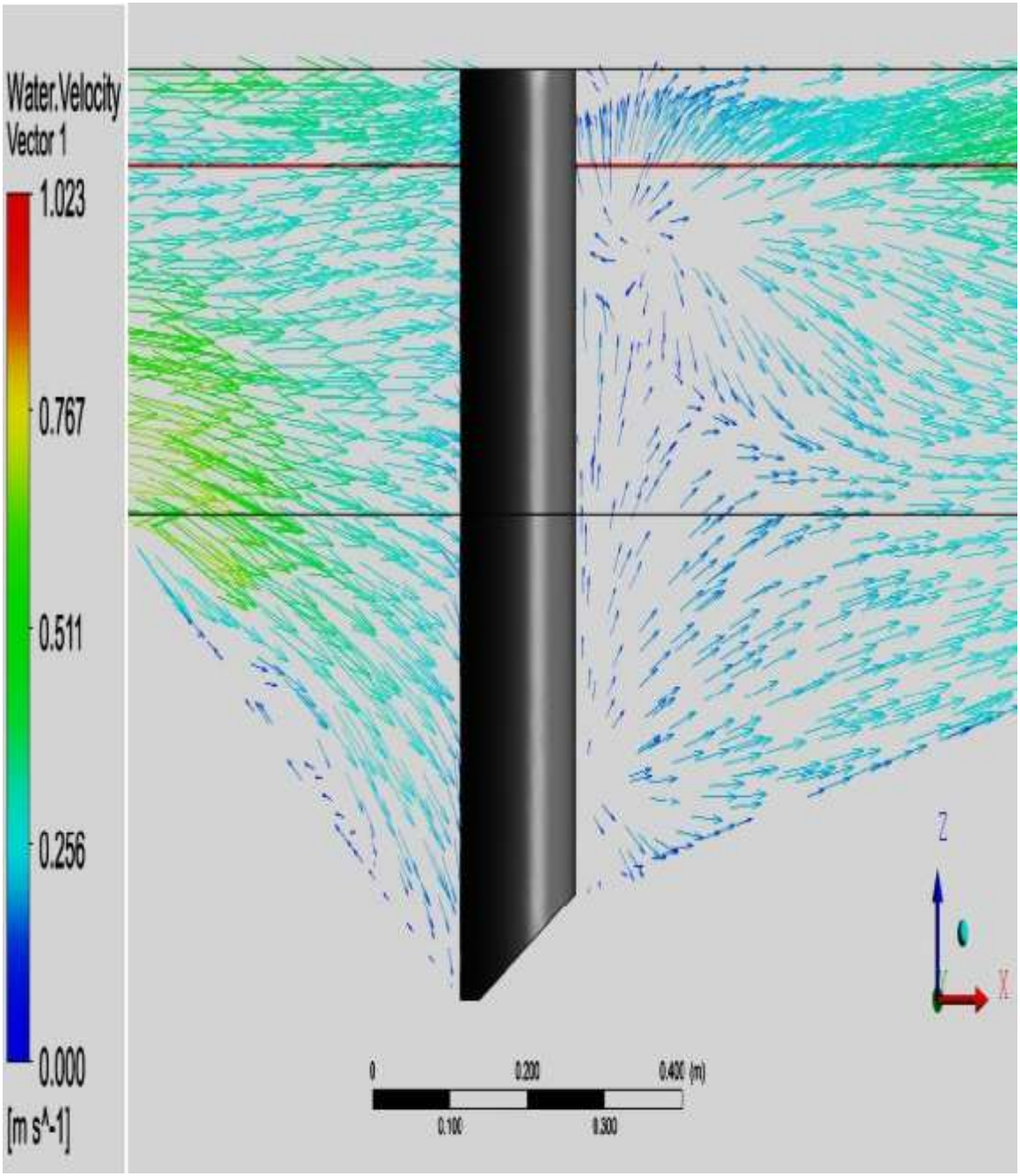

Figure 8 Velocity vectors in the plane through the channel centreline. The vectors above the red line are air velocities, where the water volume fraction is zero. The approach flow velocity is uo = 0.34 m/s.

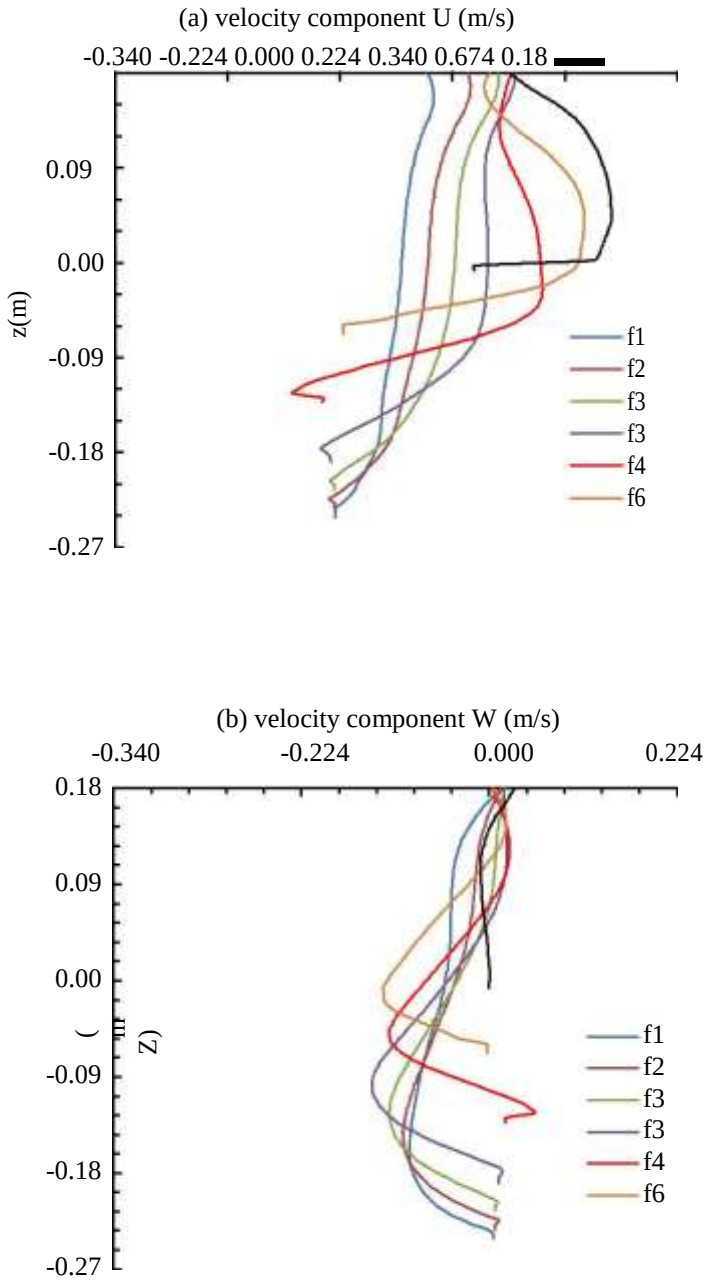

Figure 9 Vertical profiles of the longintudinal or x-component and the vertical or z-component of flow velocity at 7 selected locations upstream of the pier.

For a further examination of the vertical structures of the flow, vertical profiles of the longitudinal or x-component of flow velocity at seven locations (f1 tof7) upstream of the pier are plotted in Figure 5a. Note that locations f1 to f6 are inside the scour hole and location f7 is outside. The velocity decreases as the flow approaches the pier; the peak velocity is slightly larger than u_o at location f7, and decreases to $0.8u_o$ at location f4 and to less than $0.3u_o$ at location f1. The decrease is due to the pier in the flow path and water column deepening toward the pier.

The profile at location f4 shows the most profound vertical structure, with flow reversal near the bed. Inside the scour hole, all the profiles Figure 11 show significant negative W values or downward velocities. The downward velocity at location f3 is the strongest ($\approx 0.3u_o$). The downward velocities intensify with depth,reach a maximum at a depth in the lower water column, and then weaken toward the bed. Downstream of the pier, the longitudinal velocities are mostly positive except in the proximity of the pier (at locations b1 and b2, . In general, the velocities increase with distance toward downstream, which is particularly the case near the free surface; the increase in velocity near the bed occurs probably because the flow accelerates over the rising bed. Another feature of the profiles is that the individual profiles show an increase in longitudinal velocity with depth below 0.1 m or 0.67D. With respect to the vertical velocity W , it is upward at the free surface. At a depth of about 0.67D, W is upward in the proximity of the pier (at locations b1 and b2) but downward at short distances from the pier (locations b3 to b6).

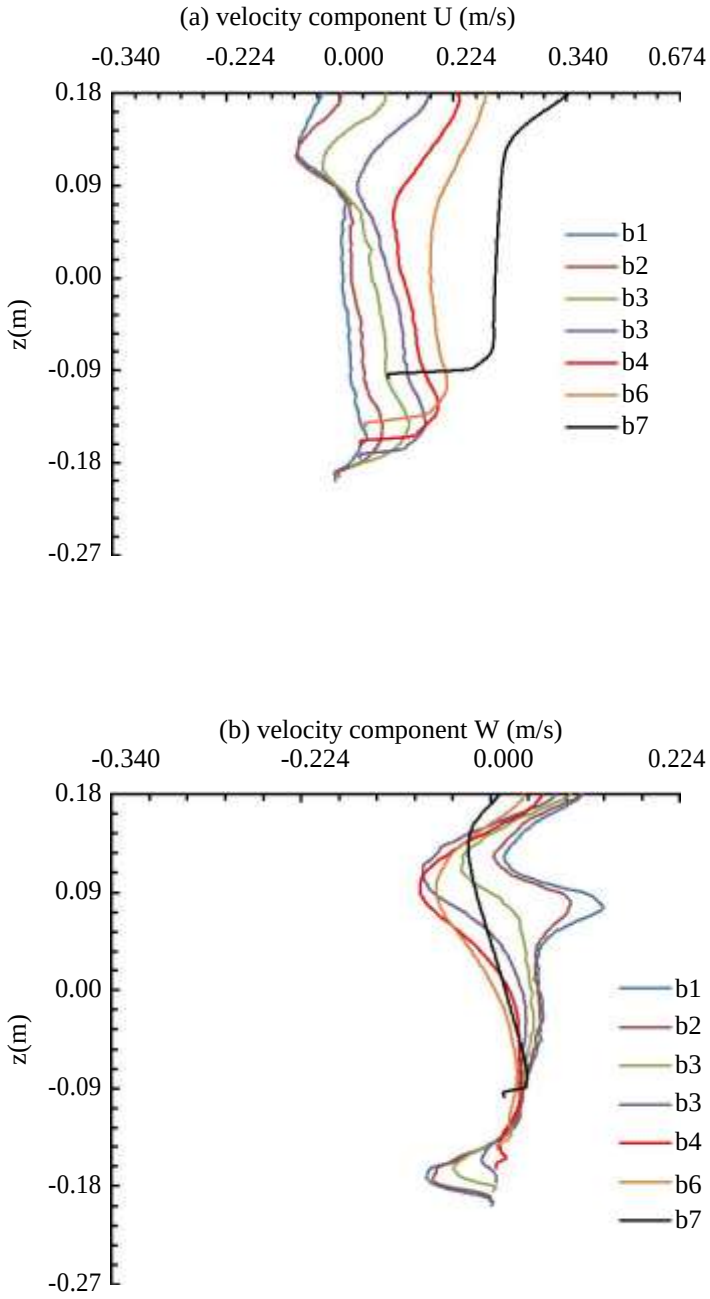

Figure 10 Vertical profiles of the x-component and z-component of flow velocity at 7 selected location downstream of the pier

4.1.5 Vorticity

Vorticity measures the tendency to form vortices or the local spinning motion of a fluid near some point. Mathematically, the vorticity vector is defined as the curl of the velocity vector field in three dimensions (U, V, W). In bridge hydraulics applications, the vorticity vector field associated with the near-bed velocity within the scour hole is the most interesting. Contours of the vorticity components in the vicinity of the channel-bed are plotted in Figures 13. In the xy-plane (Figure 13) the vertical component of the vorticity vector is relatively strong in small neighbourhoods along the outer edge of the scour hole; the values are positive to the left of component of the vorticity appears to be weak in the wake region downstream of the pier. The pier (to an observers facing downstream), meaning that fluid particles have the tendency to rotate counter-clockwise about the z-axis as seen from the top by an observer located in the neighbourhoods and travelling along with the fluid; the values are negative to the right of the pier, meaning that fluid particles there have the tendency to rotate clockwise. Relatively strong vorticity is also seen .

In the xz-plane for the y-component of the vorticity vector there is a core area of strong vorticity located in the middle of the upstream portion of the scour hole, with significant implications of sediment scouring. Since the vorticity component has negative values within the core, fluid particles there have the tendency to rotate clockwise, as seen by an observer facing in the positive direction of the y-axis .The maximum intensity ($\approx 100\ s^{-1}$) is somewhat higher than that shown in Figure 13 .The vorticity is weak outside the core area .Just behind the pier on the downstream side, the tendency to rotate around the y-axis is evident in a very small neighbourhood. Strong vorticity is observed over a very small region at the upstream and downstream edges of the scour hole.

In the yz-plane the x-component of the vorticity vector is stronger outside the scour hole than inside. The x-component of the vorticity has positive values to the right of the pier (to an observer facing downstream), meaning that fluid particles have the tendency to rotate counter-clockwise, as seen by an observer facing in the positive direction of the x-axis; the values are negative to the left of the pier, meaning that fluid particles there have the tendency to rotate clockwise.

(a) xy-plane

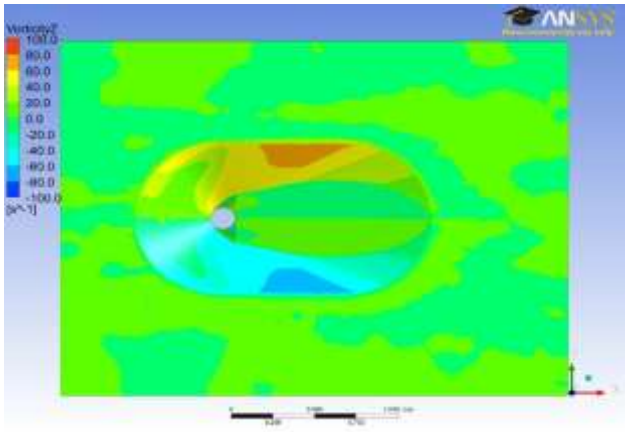

(b) xz-plane

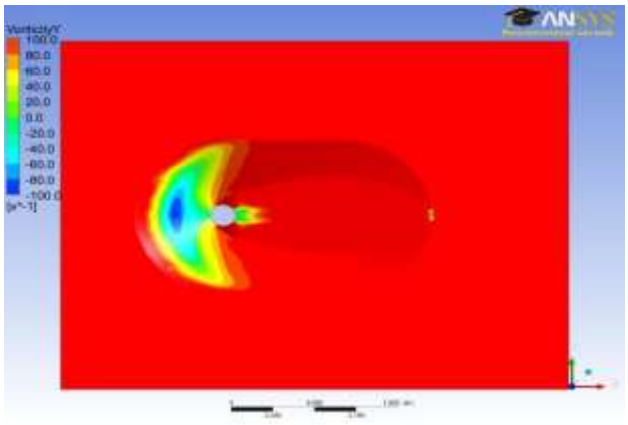

(c) yz-plane

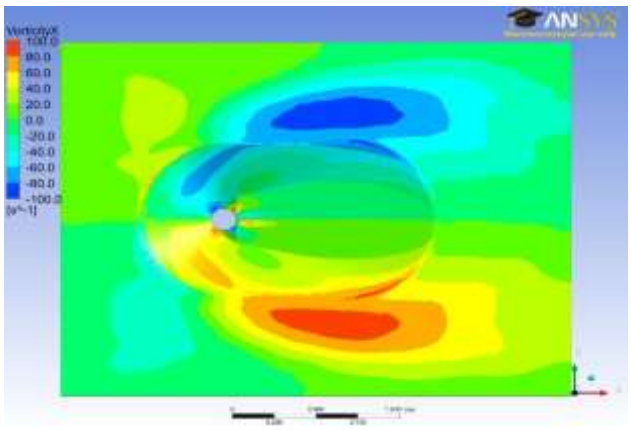

Figure 11 Contours of vorticity associated with the near-bed flow velocity: (a) the xy-plane, (b) the xz-plane, and (c) the yz-plane.

4.1.6 Turbulence intensity and bed shear stress

In fluid dynamics, turbulence kinetic energy (TKE) is the mean kinetic energy per unit mass associated with eddies in turbulent flow. Physically, the turbulence kinetic energy is characterised by measured root-mean-square (RMS) velocity fluctuations. In Reynolds-averaged Navier Stokes equations, the turbulence kinetic energy can be calculated based on the closure method, i.e. a turbulence model. Generally, the TKE can be quantified by the mean of the turbulence normal stresses.

The bed shear stress, τ_b, is an important quantity to predict in studies of scour development. The predicted τ_b values from this study compare reasonably well with experimental data of Graf and Istiarto (2002). There are some discrepancies for the area just before water enters the scour hole; the predictions show a high shear stress peak, which is not seen in the experimental data. A possible explanation is that the local mesh in the vicinity of the channel-bed are not fine enough to adequately resolve the vertical structure of the near-bed flow; it is noticed that the velocity profile shown in Figure 14 at location f7 appears to have an unrealistic shape near the bed. Using the eddy viscosity method $\tau_b = \rho v_t \partial v_{par}/\partial n$, Graf and Istiarto (2002) determined the bed shear stress from laboratory measurements of flow velocity, where v_{par} is a velocity parallel to the bed based on longitudinal and vertical components of flow velocity, n is the normal distance from the bed surface to the position where the velocity components are measured, and v_t is the eddy viscosity taken as 1.3×10^{-4} m^2/s. The specific Reynolds shear stresses, τ_{13}, at 14 locations upstream and downstream of the pier in the plane through the channel centerline are plotted as vertical profiles. Upstream of the pier, τ_{13} remains approximately linear outside the scour hole (the solid black curve at location f7, showing little vertical variations); all the other profiles show large variations near the bed, the f4 profile being the most dramatic (Figure 14). Downstream of the pier, τ_{13} has relatively high values near the surface and near the bed; overall the τ_{13} values are lower than those upstream of the pier.

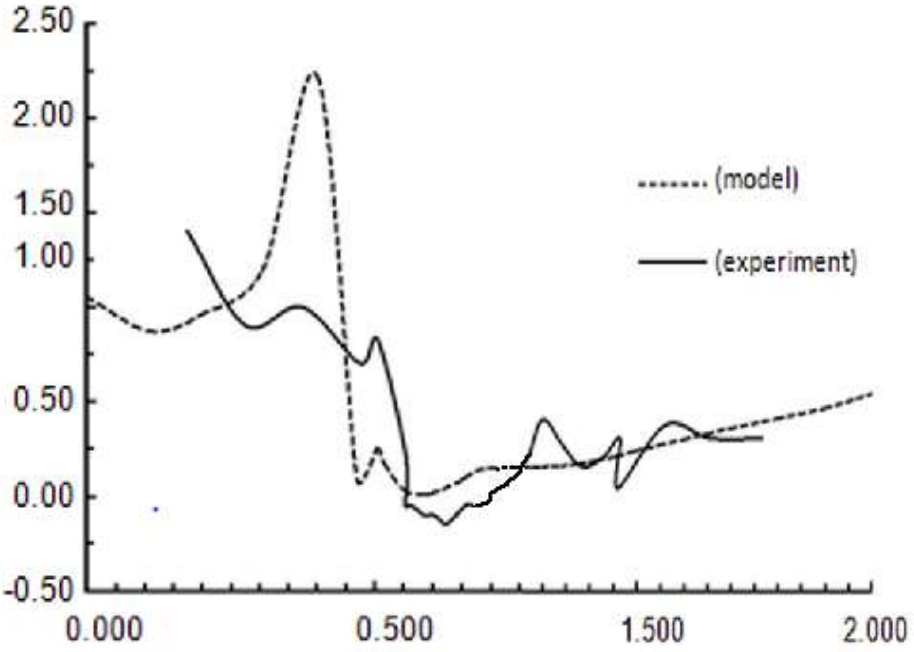

Figure 12 A comparison of the bed shear stress between model prediction and experimental data.

The vertical distributions of the turbulence kinetic energy, ,normalised by the shear velocity, $u_* \equiv (\tau_b/\rho)^{0.4}$, are plotted in Figure 14 for two planes 0.2 m or 1.33D upstream and downstream of the pier. The value for $u_*$was reported as 2.64 cm/s in Graf and Istiarto (2002). The normalised k/u_* values aresmall from the free surface down to a depth of 2D, both upstream and downstream of the pier. The k/u_* values increase by six-fold near the bed upstream of the pier. Downstream of the pier, relatively speaking, k/u_* has higher values near the surface possibly in association with flow separation

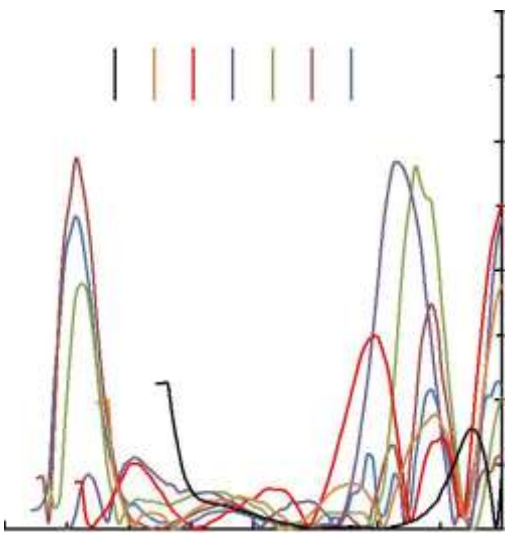

Depth below the free surface z(m)

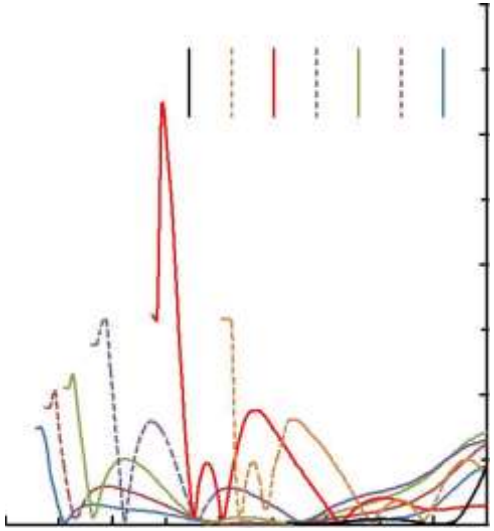

Depth below the free surface, z(m)

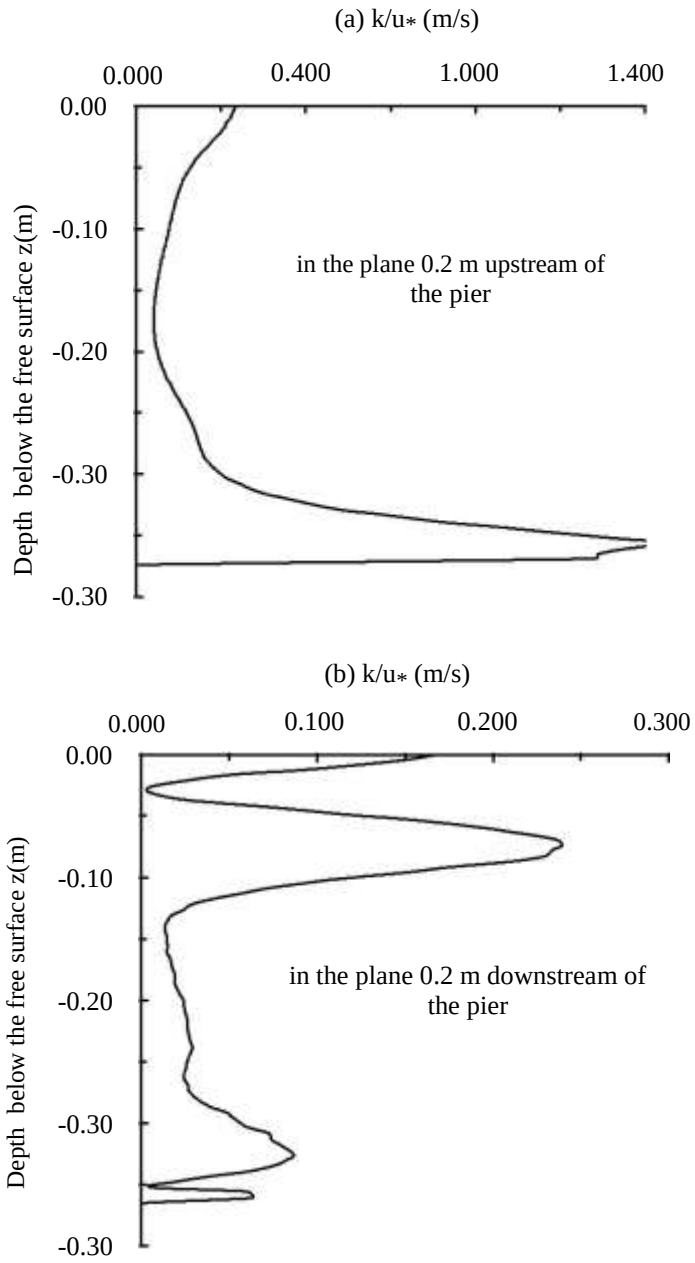

Figure 13 Distributions of normalized turbulence kinetic energy in two representative planes.

4.2 The SPH model

4.2.1 Sensitivity test simulations and approach flow

Test simulations were carried out for three purposes: (a) to ensure that the inflow to the main channel or the approach flow is consistent with that in Graf and Istiarto's (2002) experiments, i.e. the inflow is steady for a certain period of time, and has a depth-averaged velocity of 0.34 cm/s and a depth of 0.18 m; (b) to confirm that the reduction in width of the main channel to increase computational efficiency does not have significant artificial effects on the flow field in the scour hole; (c) to ensure that the installation of an artificial lid on the top of the main channel does not result in unrealistic velocity profiles between the water surface (in the experiments) and the channel-bed. The SPH method has a number of fundamental features. A set of particles possessing individual material properties represent the state of a system. These particles move according to governing conservation equations. Since its development for astrophysical problems (Lucy, 1977; Gingold and Monaghan, 1977), this method has been extensively studied and extended to dynamic fluid flows with large deformations. The key features of the method are summarised below

Consistent inflow has successfully been produced by systematically adjusting the dimensions of the upstream reservoir fluid volume, distance between smoothed fluid particles and some of the parameters listed in Table 3.2. As illustrated by the time series of flow velocities . the inflow becomes quasi-steady after 100 time steps and remains steady over a sufficiently long time period (say between time steps 100 and 200). At the middle depth (0.09 m above the channel-bed in a 0.18 m water column), the inflow has a velocity of 0.341 m/s, which is very close to the approach flow velocity in the experiments.

The use of the weighted average over the neighbouring particles for stability i.e implies the smoothed approximation nature for hydrodynamics problems. The adaptable nature of the method is achieved at a very early stage of the field variable approximation which is performed at each time step based on a current local set of arbitrary distributed particle. The method does not require a pre-defined mesh system to provide any connection within the particles in the process of computation and works efficiently without any particle refinement operation.

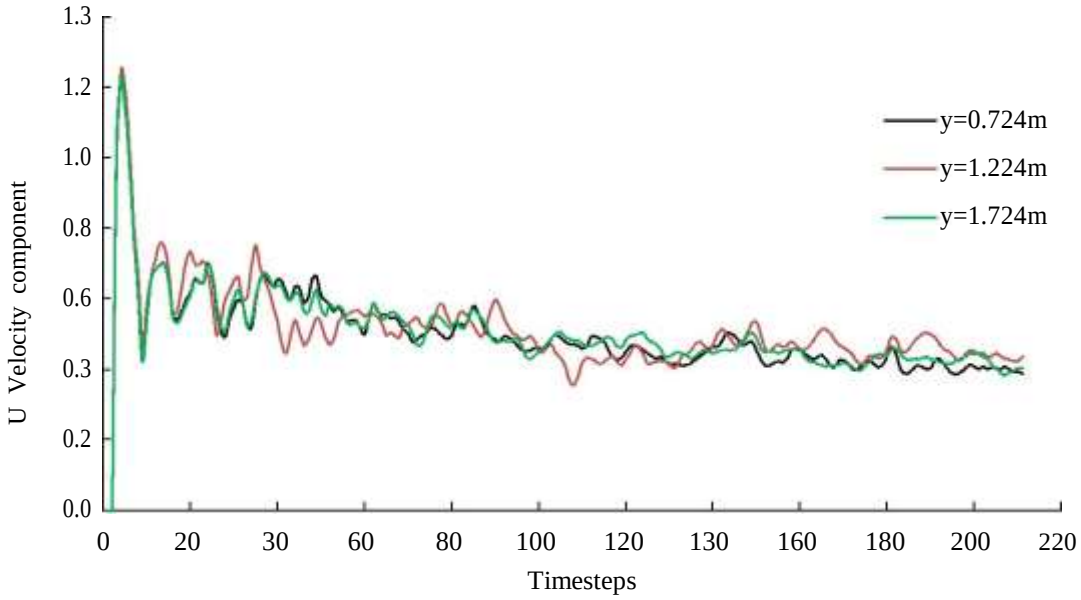

Figure 14 Time series of longitudinal flow velocities at three different locations below the gate of the upstream reservoir . The z coordiates of these locations are 0.09 m (or 0.09 m above the channel-bed).

An examination of the model results (not shown) for a number of test simulations, where the main channel had different widths, shows no significant effects on the velocity field upstream and downstream of the scour hole in the main channel and within the scour hole around the pier. Thus, 4D was taken as the width on both sides of the pier.Through test simulations, it has been confirmed that predicted velocity profiles do not have unrealistic shape in the presence of an artificial lid on the top of the main channel. From the peak velocity location which represents the free surface in the experiments, to the channel-bed, the flow velocity decreases with increasing distance below the water surface. The profiles show a velocity of 0.341 m/s at the middle depth (z = 0.09 m), with the depth-averagedvelocity matching well the experimental condition in Graf and Istiarto (2002). Therefore, it was concluded that the SPH model has been properly setup for the application.

Note that similar to FEM simulations, all the SPH simulations begin from a state of rest. Initially, the model channels, including the main channel and downstream channel extension, are filled with water. The use of this initial condition, along with the use of a lid, helps force water entering the scour hole and flowing around the pier , which is difficult to achieve in dam-break type of simulations. In the following, SPH results were presented at time step 198 or 4.93 s of model time.

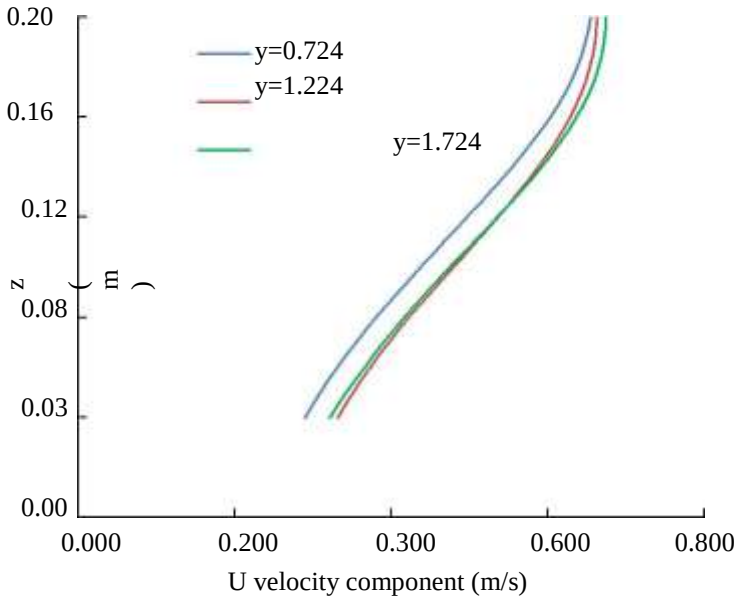

Figure 15 Vertical distributions of longitudinal velocity at three locations below the gate at the time step 198 or at 4.93 s of model time. The data gap in the bottom 3 cm distance is due to SPH limitation with respect to solid boundaries.

4.2.2 Velocity vector field in the horizontal plane

Velocity vectors in the horizontal plane at the mid-depth (or z = 0.09 m) are shown in Figure 2. It is possible to make a number of observatons: (a) Water flow passing though the gate (at x = 0 m) reamains parallel in a straightline to the channel-bed (not covered in Figure 2) except in regions near the two sidewalls (at y = 0.30 and 2.04 m, respectively), where the flow direction shows some variation from the straight path; (b) near the upstream nose of the pier, flow velocity changes in both magnitude and direction; (c) some circulations due to wake vortices are visible just downstream of the pier; (d) further downstream, velocity vectors regain uniformity (the figure does not cover that far downstream).

4.2.3 Velocity vector field in the vertical plane

In Figure 19, a plot of velocity vectors in the vertical plane along the centreline of the main channel . As the inflow results from a sudden lifting of the gate (somewhat like a dam-break), velocity vectors just downstream of the gate are not perpendicular to the gate . Water flows though the main channel and enters the scour hole, where velocity vectors have a downward component. As the flow approaches the pier, a down flow occurs just upstream of the pier. Downstream of the pier, the flow weakens with small velocities at different directions. Further downstream in the scour hole, the velocity vectors are more or less parallel to the local rising bed profile and accelerate.

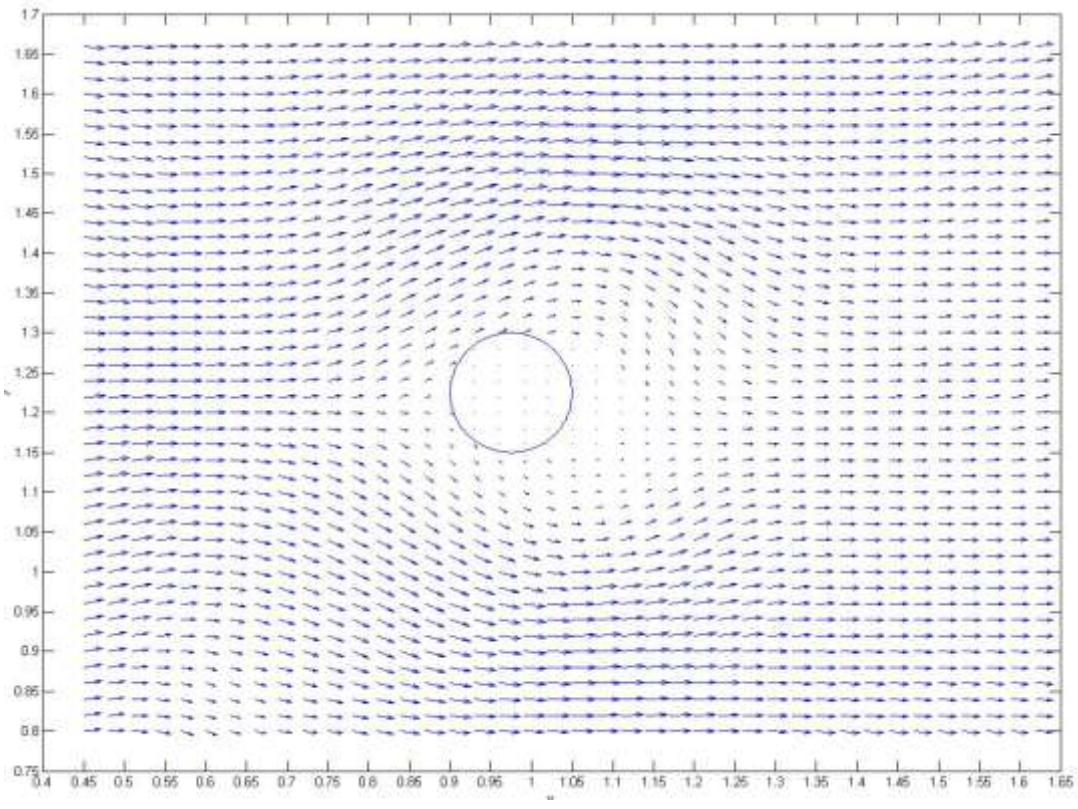

Figure 16 A horizontal plane showing velocity vectors at a depth of 0.09 m below

4.2.4 Vertical profile of longitudinal velocity

Vertical profiles of the longitudinal velocity obtained from SPH simulations at seven locations upstream of the pier are plotted in Figure 20. The velocity decreases as the flow approaches the pier. The decrease is because of the pier being in the flow path and results in downward motions. The profiles at locations f4, f6 and f7 show more profound vertical structures. Inside the scour hole, all the profiles show negative values for the vertical component of velocity W or downward velocities. The downward velocity at location f4 is the strongest ($\approx 0.36u_o$ as the maximum). The downward velocities intensify with depth,reach a maximum at the middle depth and then weaken towards the channel-bed.

The velocity profile outside the scour hole at location f7 shows weak upward velocities.Downstream of the pier, longitudinal velocities are positive. In general the velocities increase with distance toward downstream, which is particularly the case near the free surface. As the flow accelerates over the rising channel-bed, velocity near the bed increases probably.

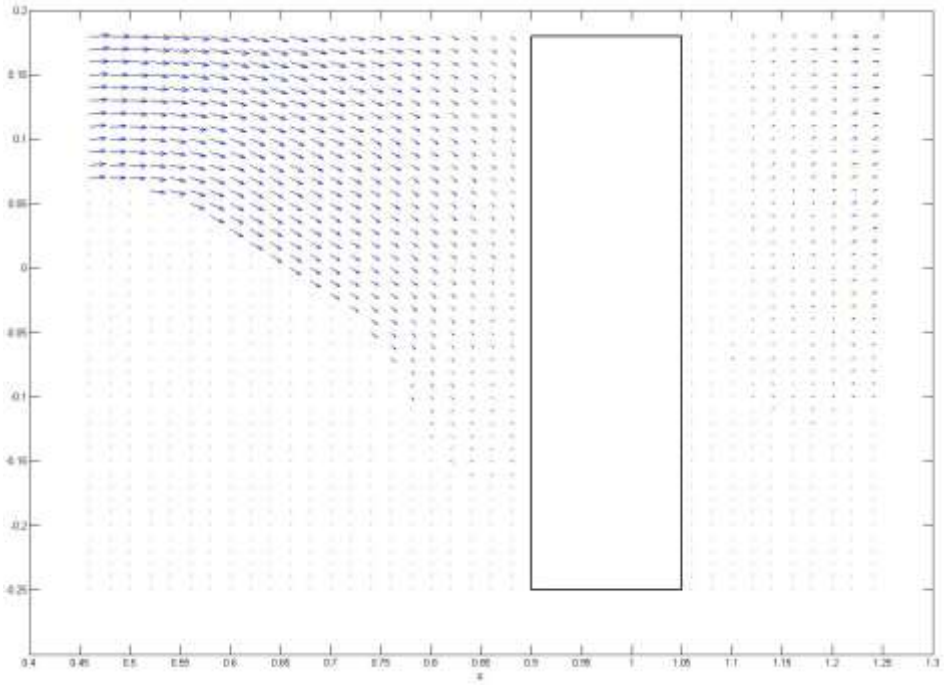

Figure 17 Velocity vectors in the vertical plane through the channel centreline.

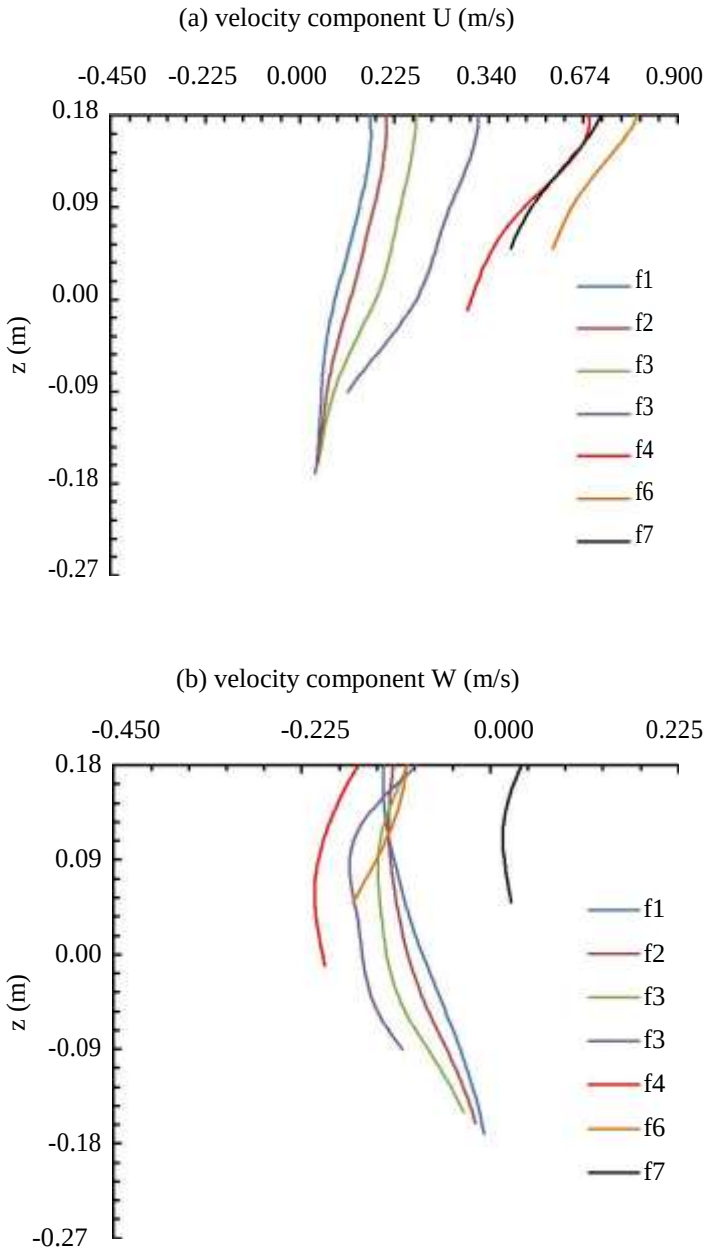

Figure 18 Vertical profiles of the x-component (panel a) and z-component (panel b) of velocity at seven selected locations (labeled as f1 to f7 in upstream of the pier. In the approach channel, the channel-bed is located at z = 0 m.

(a) velocity component U (m/s)

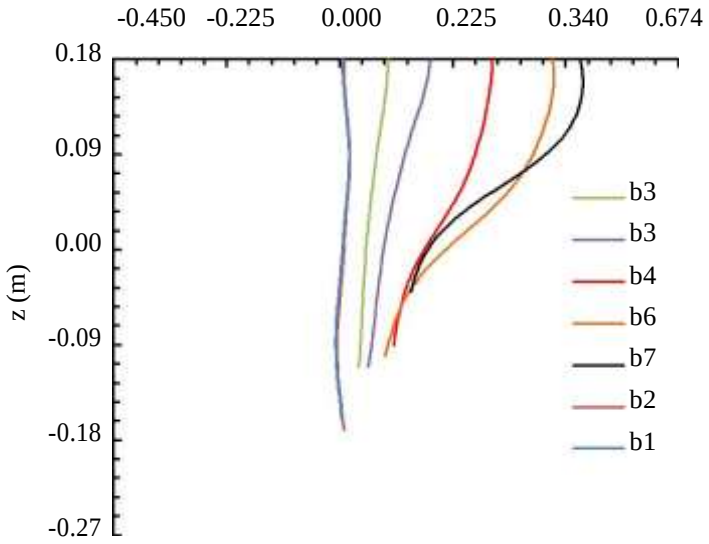

(b) velocity component W (m/s)

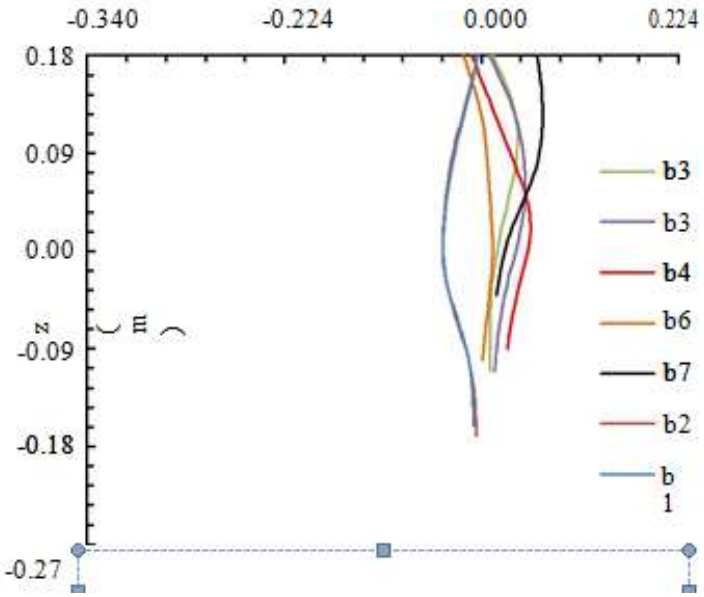

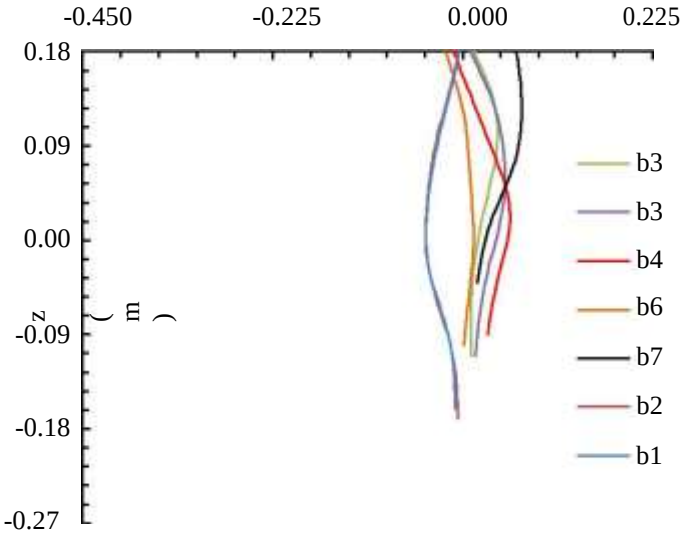

Figure 19 Vertical profiles of the x-component (panel a) and z-component (panel b) of velocity at 7 selected locations (labeled as b1 to b7 downstream of the pier. In the approach channel, the channel-bed is located at z = 0 m.

4.2.5 Comparison between FEM and SPH

FEM, a mesh-based hydrodynamics model, and SPH, a mesh-free hydrodynamics model, have been applied to the bridge hydraulics problem of free-surface flow around a circular pier in a fixed scour hole. In FEM, the built-in Design Modeler within the ANSYS workbench was really a user-friendly tool to build the geometry with provisions of making lots of modification. This makes it easier to create the complex geometry precisely. On the other hand, in SPH, the geometry was developed with other available drawing or geometry development tools.

4.3 Comparison of vertical profiles between SPH, FEM and experiments

In Figure 23, vertical profiles of the longitudinal velocity from both SPH and FEM simulations at the seven locations (f1 to f7, Figure 3) upstream of the pier arecompared with laboratory measurements (Graf and Istiarto, 2002). The comparison appears to be reasonable, especially at locations f1, f2, f3 and f3 near the pier . At location f7 outside the scour hole, both the model predicted velocities are too large, compared to measurements. At the location f6 near the upstream edge of the scour hole, predicted velocities from SPH are larger than FEM simulated velocities and experimental measurements.

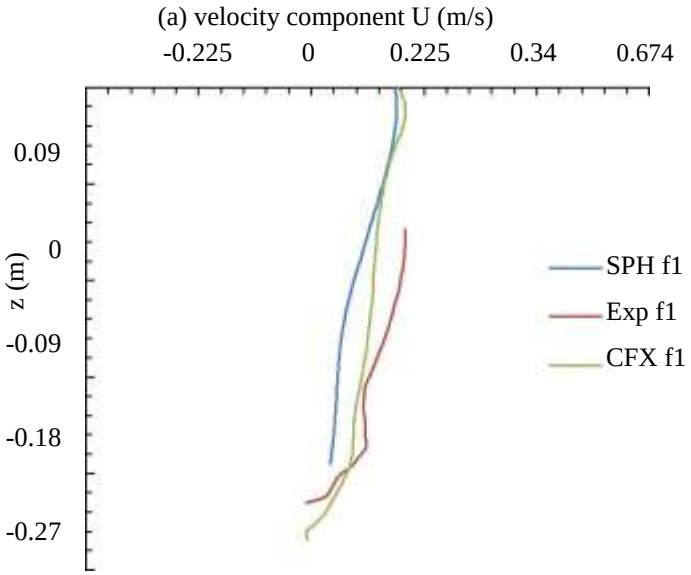
(a) velocity component U (m/s)
-0.225
0
0.225
0.34
0.674
0.09
0
-0.09
-0.18
-0.27
z (m)
SPH f1
Exp f1
CFX f1

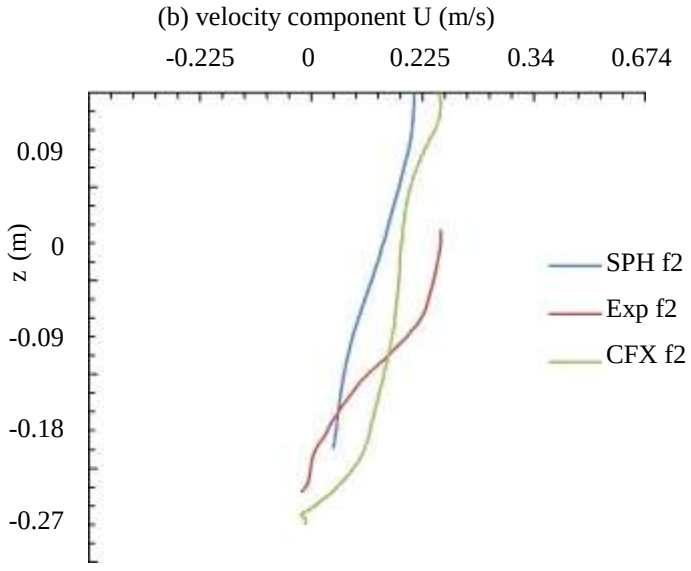
(b) velocity component U (m/s)
-0.225
0
0.225
0.34
0.674
0.09
0
-0.09
-0.18
-0.27
z (m)
SPH f2
Exp f2
CFX f2

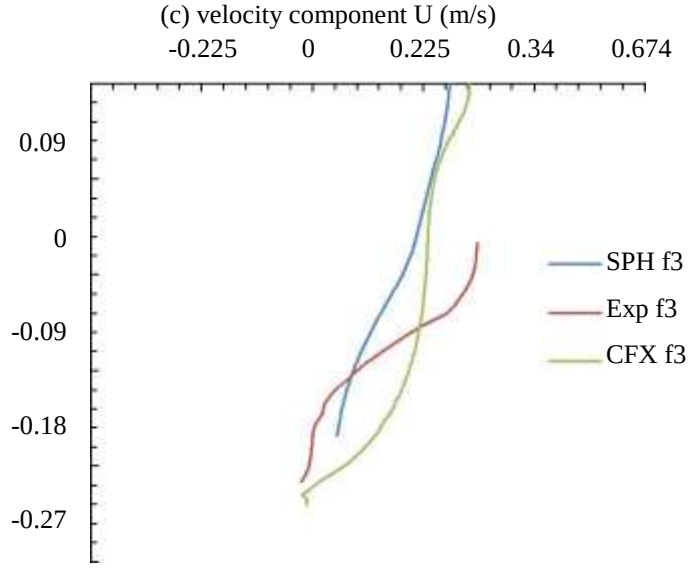
(c) velocity component U (m/s)
-0.225
0
0.225
0.34
0.674
0.09
0
-0.09
-0.18
-0.27
SPH f3
Exp f3
CFX f3

(d) velocity component U (m/s)

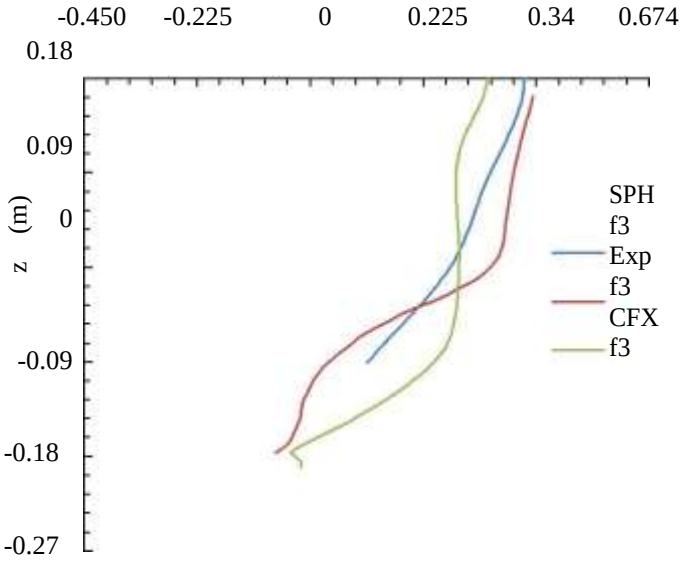

(e) velocity component U (m/s)

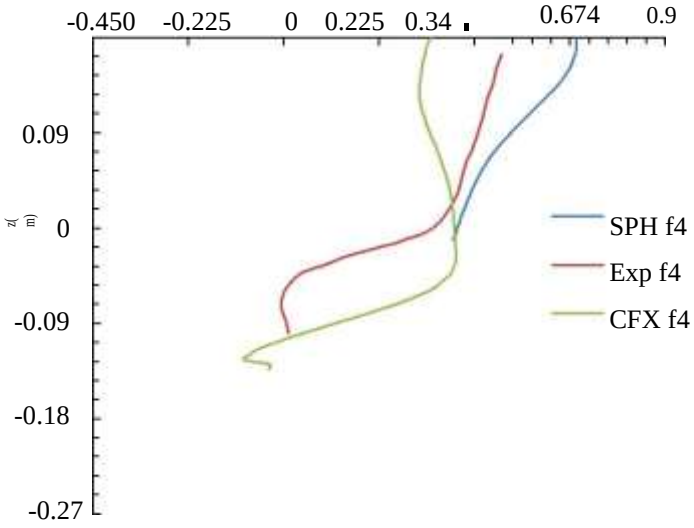

(f) velocity component U (m/s)

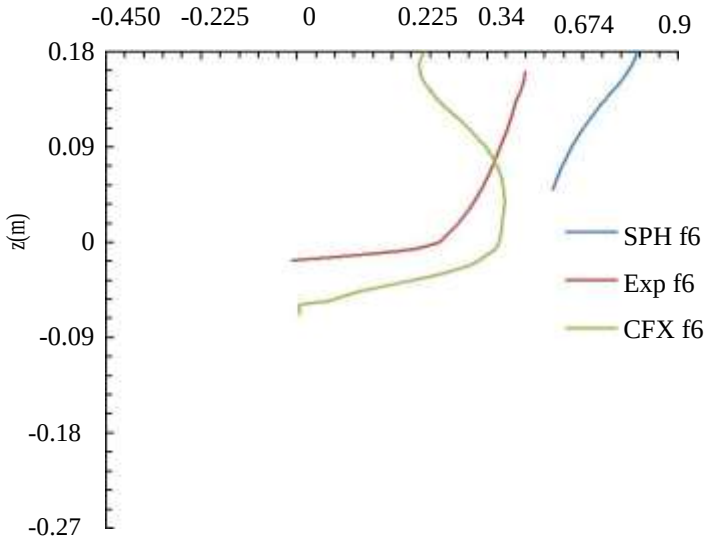

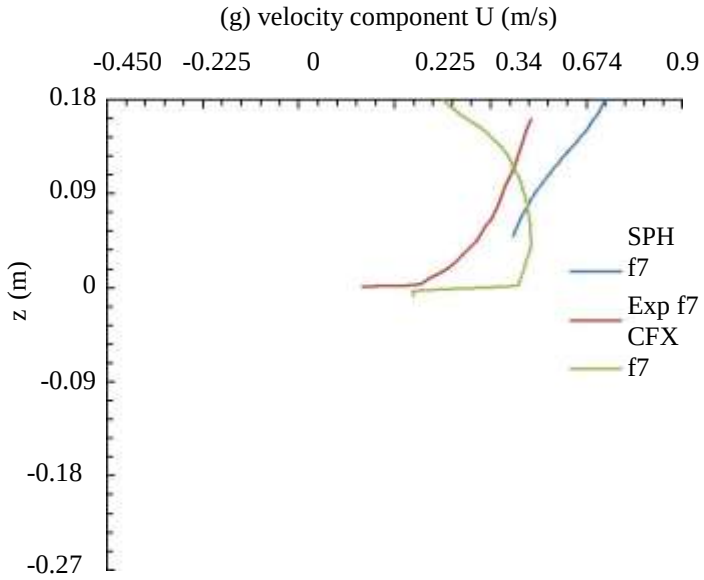

Figure 20 Comparison of the longitudinal velocity among FEM, SPH

For simulations using FEM, a mesh size should be defined with a proper selection of mesh type and other control features. This brings the inaccuracy in the sense that with a coarser mesh, near-boundary complex flow features are impossible to predict. In other words, one losses the near-boundary flow features when using a coarser mesh. In principle, one may use a finer mesh size to adequately resolve the near-boundary flow, but the required overall computational memory increases significantly, which makes it computationally inefficient. In this case, application of inflation layers in the boundary mesh resolves some part of the near-boundary flow. On the contrary, SPH does not need any mesh as it is a mesh-free method. The flow field in SPH is associated with the trajectory of each particle. Therefore there is no numerical diffusion, which is advantageous over mesh-based methods.

(a) velocity component W (m/s)

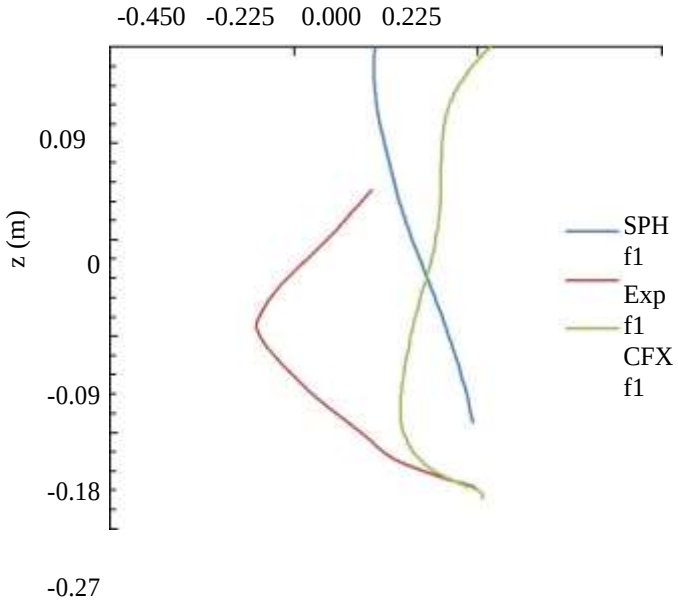

(b) velocity component W (m/s)

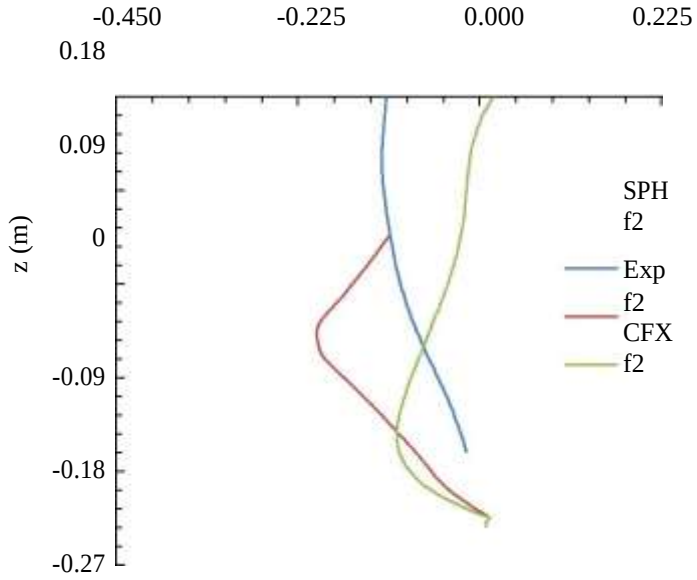

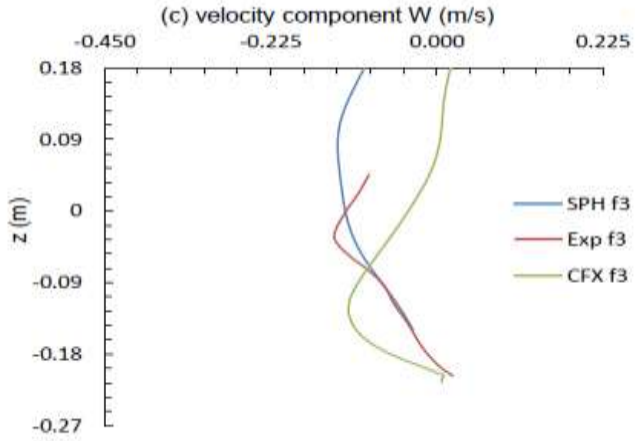

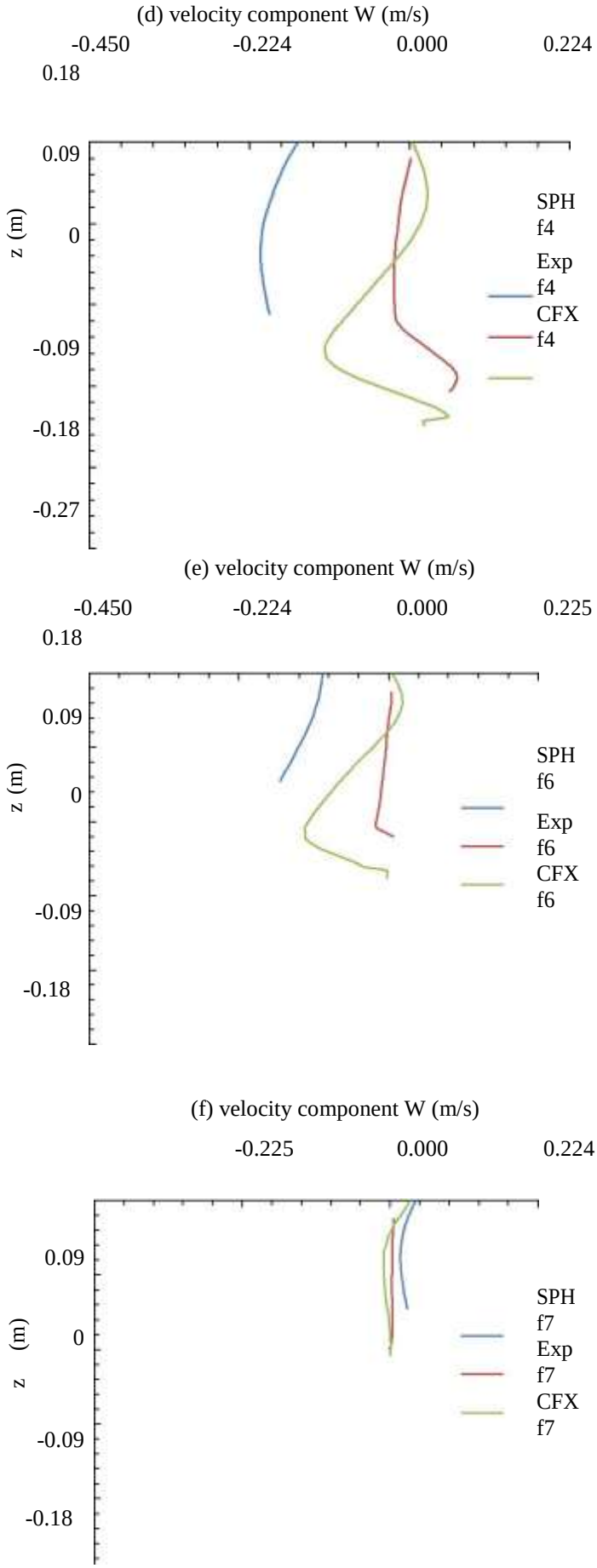

Figure 21 Comparison of the vertical velocity among FEM, SPH and experimental measurements (Graf and Istiarto, 2002) at selected locations upstream of the pier.

(a) velocity component U (m/s)

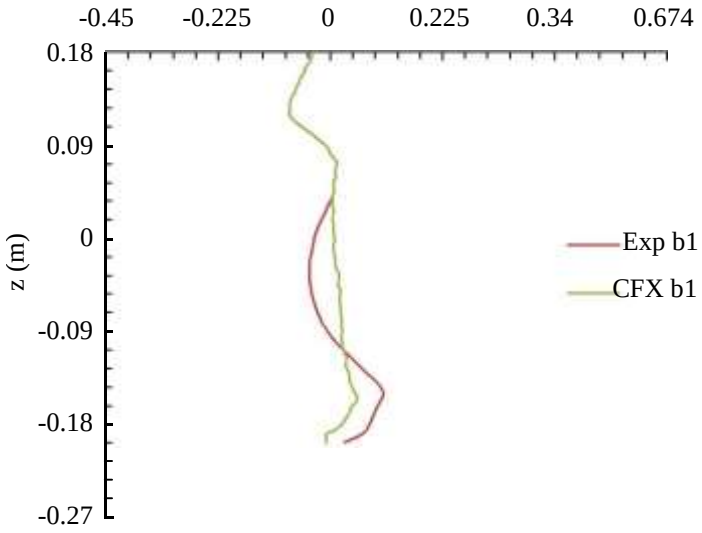

(b) velocity component U (m/s)

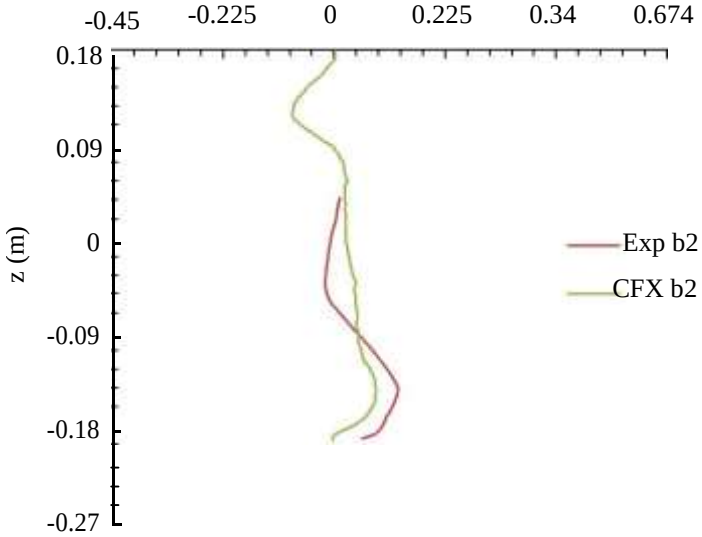

(c) velocity component U (m/s)

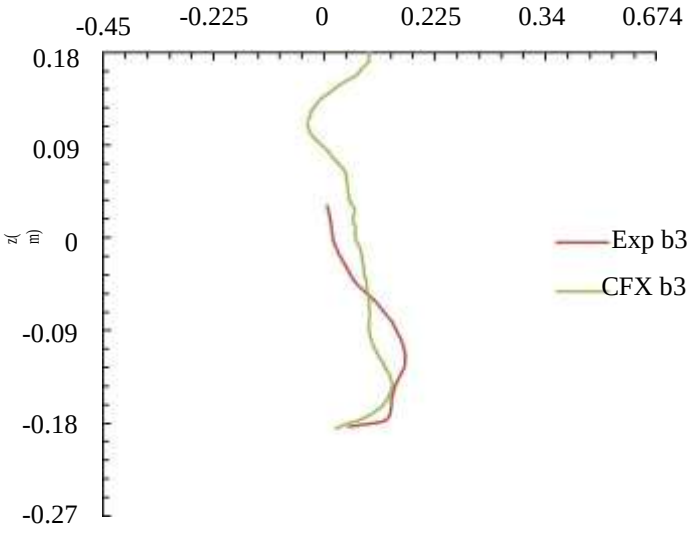

(d) velocity component U (m/s)

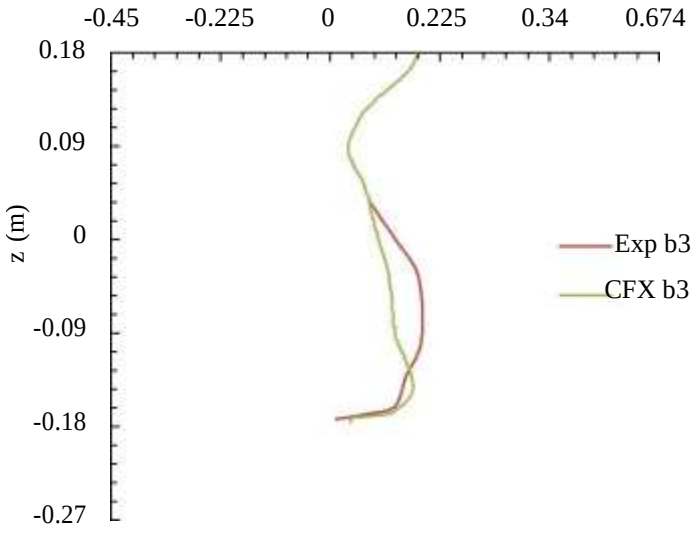

(e) velocity component U (m/s)

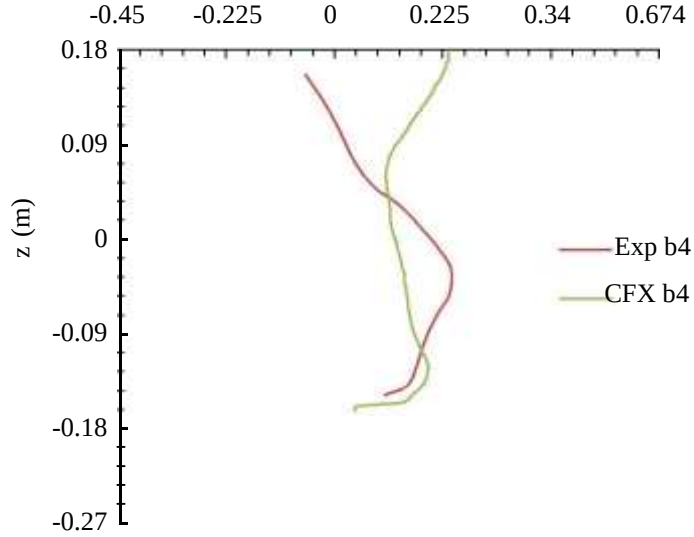

(f) velocity component U (m/s)

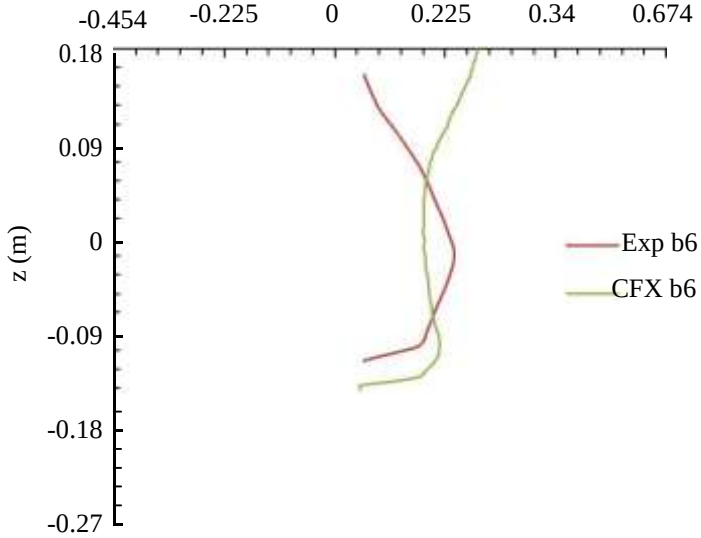

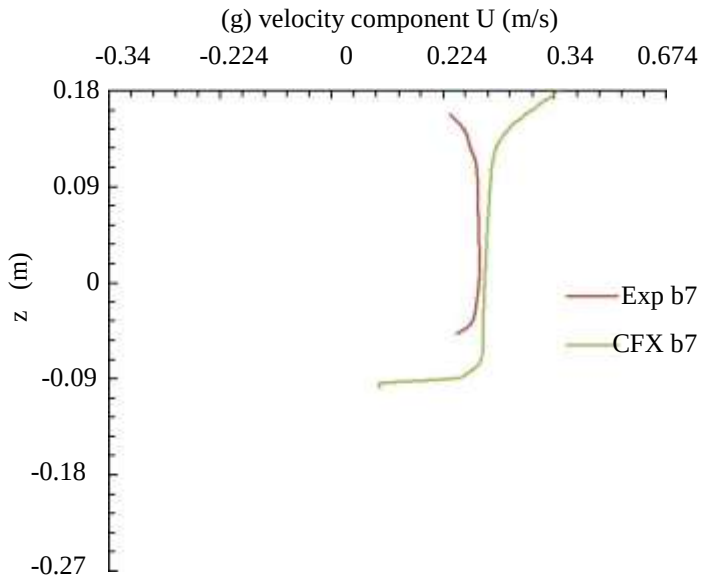

Figure 22 Comparison of the longitudinal velocity among FEM and experimental

In application of SPH to the bridge hydraulics problem using the existing SPH code, it was not possible to specify uniform inflow at the entrance or inlet of the main channel. In FEM, there are different choices of inflow condition specification. Based on the results presented in Sections 4.1 and 4.2, FEM appears to be more robust in determining the flow within the scour hole and around the pier. FEM prediction is shown to capture some detailed features of the flow field in a realistic manner, including strong vortices at the foot of the pier on the upstream side, and eddy motions in the wake region. These details are absent from the SPH results. Two possible reasons are: (a) the use of an artificial lid on the top of the model channel in order to force particles to reach deeper in the scour hole; (b) the use of a relatively large distance between particles so as to maintain manageable computational costs. Eddy motions of length scale shorter than the distance cannot be resolved. The velocity vectors and vertical velocity profiles based on FEM simulation output have shown vortices and eddy motions of different length scale commendably. Also, FEM has been computationally more efficient than SPH; FEM needed less computational time to produce results for the given conditions in this modelling research. SPH needs modification for application to the bridge hydraulics problem.

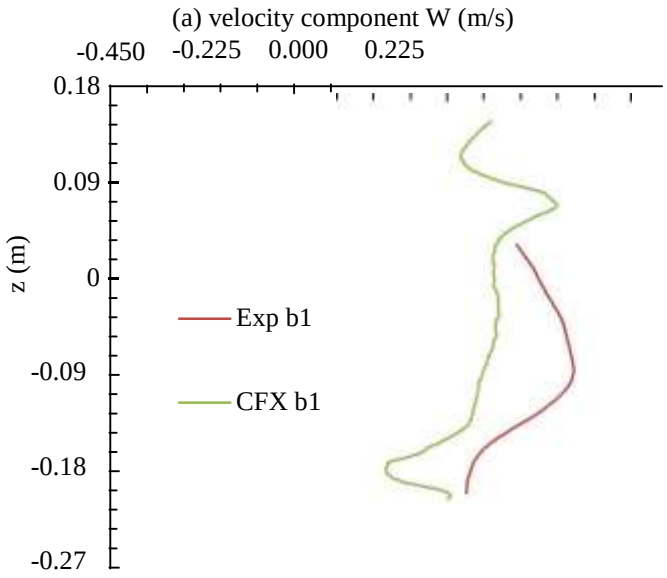
(a) velocity component W (m/s)
-0.450
-0.225
0.000
0.225
0.18
0.09
0
-0.09
-0.18
-0.27
z (m)
Exp b1
CFX b1

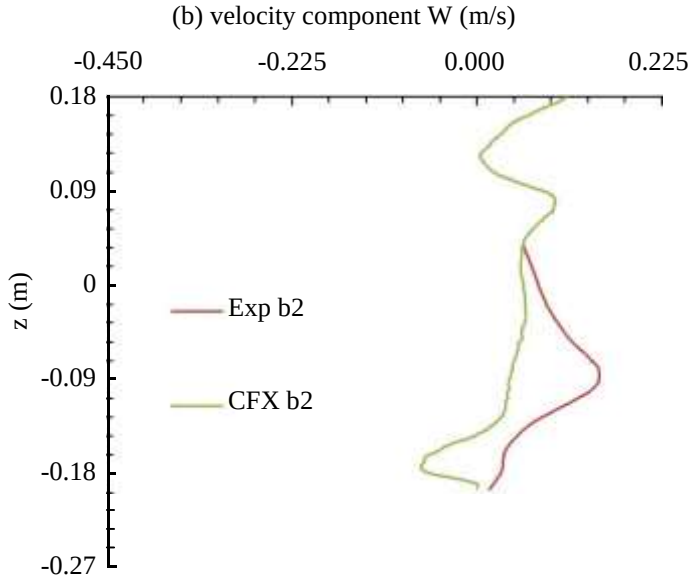
(b) velocity component W (m/s)
-0.450
-0.225
0.000
0.225
0.18
0.09
0
-0.09
-0.18
-0.27
z (m)
Exp b2
CFX b2

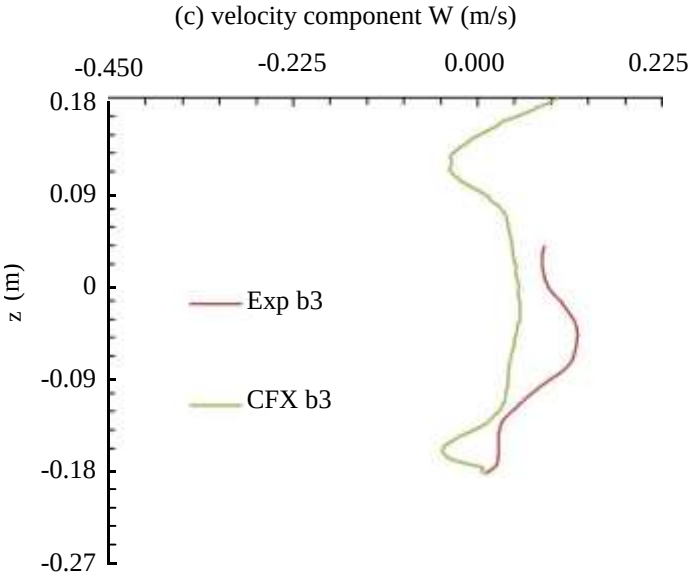
(c) velocity component W (m/s)
-0.450
-0.225
0.000
0.225
0.18
0.09
0
-0.09
-0.18
-0.27
z (m)
Exp b3
CFX b3

(d) velocity component W (m/s)

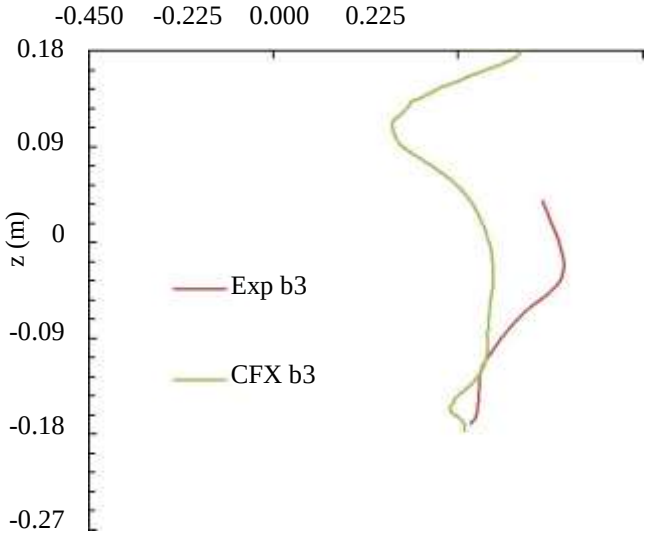

(e) velocity component W (m/s)

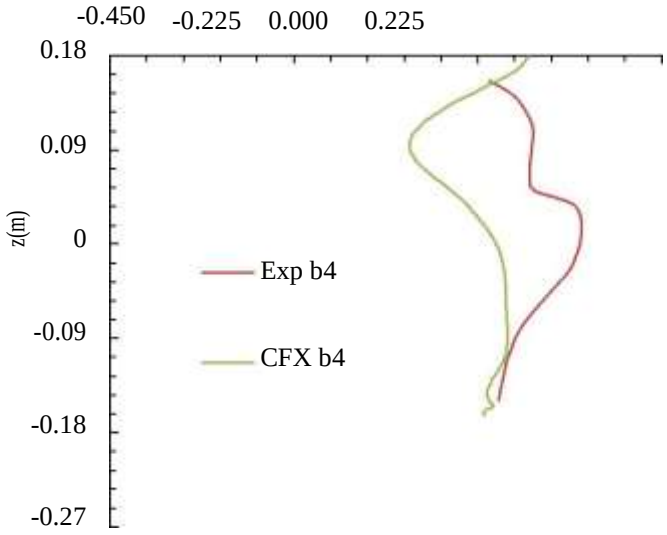

(f) velocity component W (m/s)

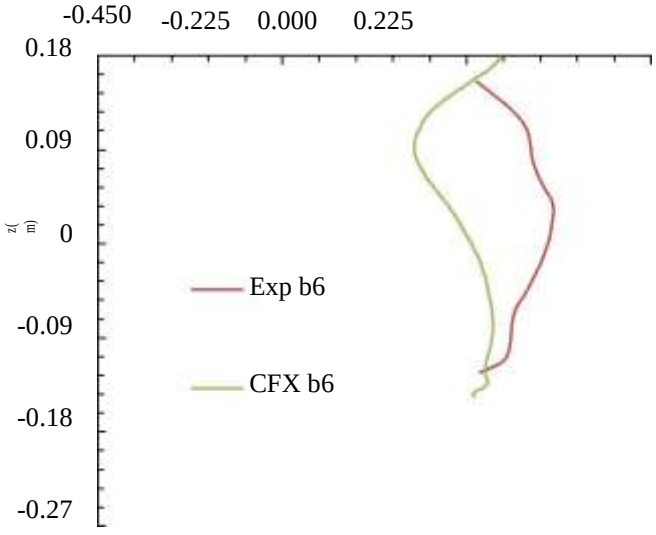

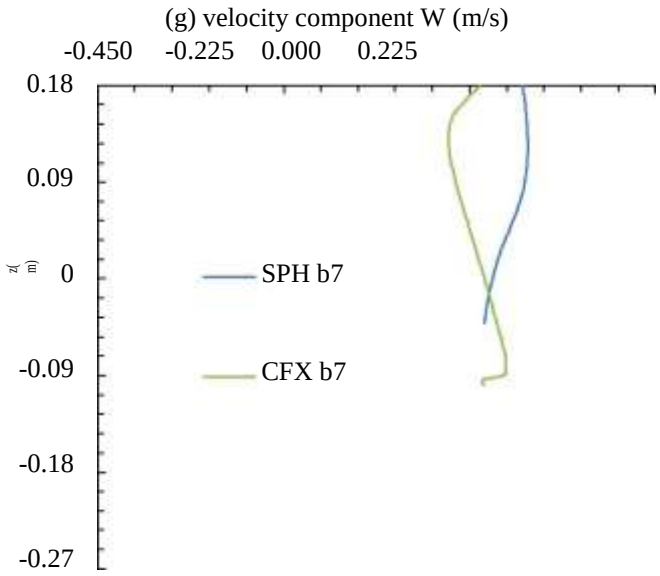

Figure 23 Comparison of the vertical velocity among FEM and experimental

5 Chapter : Conclusion

5.1 Concluding remarks

River flow has caused significant bridge pier scour, and resulted in many bridge failures. This research focuses on the problem of scour-inducing turbulent flow passing around a circular pier in a fixed scour hole. For given hydraulic conditions and geometric parameters, numerical prediction of the flow field has been obtained with FEM, a mesh-based hydrodynamics model. SPH, a mesh-free hydrodynamics model has also been applied for the same hydraulic conditions and geometric parameters as a complementary. The prediction from FEM model is in reasonable quantitative comparison with available laboratory measurements (Graf and Istiarto, 2002). An analysis of the results from the two numerical models leads to the following conclusion:

(1) FEM prediction is shown to capture some detailed features of the flow field in a realistic manner, including strong vortices at the foot of the pier on the upstream side, and eddy motions in the wake region. These details are absent from the SPH results. Two possible reasons are: (a) the use of an artificial lid on the top of the model channel in order to force particles to reach deeper in the scour hole; (b) the use of a relatively large distance between particles so as to maintain manageable computational costs. Eddy motions of length scale shorter than the distance cannot be resolved.

(2) Prediction of bed shear stress as direct output from FEM agrees well with the measurements. Some discrepancies exist for locations just before water enters the scour hole. FEM prediction of the near-bed turbulence kinetic energy is realistic. These predictions are useful for the calibration of sediment transport models.

(3) On the basis of FEM simulations, downstream of the pier, flow separation and complex vortex stretching take place but appear to be confined to the upper water column. This finding is new. The confinement may be explained as follows: Downstream of the pier, the near-bed flow accelerates over the rising bed, which would create a favorable pressure gradient and therefore tends to

suppress flow separation. Clockwise and counter-clockwise wake vortices in the horizontal are visible over a large distance (many times the pier diameter) from the pier.

(4) On the basis of FEM simulations, upstream of the pier, the turbulent kinetic energy increases by six-fold near the bed from the value near the free surface. Downstream of the pier, the turbulent kinetic energy has higher values near the free surface than near the bed, possibly due to flow separation in the upper water column.

(5) Both models predict a downflow near the upstream nose of the pier. This prediction is supported by the measurements. Comparisons between predicted and measured velocity profiles at a series of locations upstream of the pier are acceptable. The downflow has important implications for the safe design of pier foundations.

5.2 Suggestion for future research

This study has used uniform approach flow in FEM simulations. Future studies should consider the influence of distributed flow velocities at the inlet and remove the assumption that the energy coefficient is unity. In the setup of SPH simulations, this study has treated the approach flow as a dam break scenario. Future SPH modelling studies should improve the specification of approach flow for application to bridge hydraulics problems. Also SPH modelling with implementation of turbulence closure schemes is expected to give more accurate measure of turbulence and flow field within the scour hole around bridge pier. More laboratory and field measurements of flow velocity around bridge piers will be useful for validation of both mesh-based and mesh-free models.

6 References

1. Ahmed, F. and Rajaratnam, N. (1998) “Flow around bridge piers.” *Journal ofHydraulic Engineering*, ASCE, 23:288-300.

2. Ali, K. H. M., Karim, O. A. and Connor, B. A. (1997) “Flow patterns around bridge piers and offshore structures.” *Proceedings of Water Resources EngineeringConference*, ASCE, San Francisco, USA, 208–213.

3. ANSYS, Inc. (2011) *ANSYS CFX-Solver Theory Guide*, Release 13.0, Southpointe, Canonsburg, PA, USA.

4. Beheshti, A.A. and Ataie-Ashtiani, B. (2010) “Experimental study of three-dimensional flow field around a complex bridge pier.”*Journal of EngineeringMechanics*, ASCE, 136:133-143.

5. Breusers, H. N. C., Nicollet, G. and Shen, H. W. (1977) “Local scour around cylindrical piers.”*Journal of Hydraulic Research*, 14:211-242.

6. Chang, T., Kao, H., Chang, K. and Hsu, M. (2011) “Numerical simulation of shallow-water dam break flows in open channels using smoothed particle hydrodynamics.”*Journal of Hydrology*, Elsevier, 308: 78-90.

7. Crespo, A.J.C., Gomez-Gesteira, M. and Dalrymple, R.A. (2007) “3D SPH Simulation of large waves mitigation with a dike.”*Journal of HydraulicResearch*, IAHR, 34(4):631-632.

8. Crespo, A.J.C., Gomez-Gesteira, M. and Dalrymple, R.A. (2008) “Modeling Dam Break Behavior over a Wet Bed by a SPH Technique.”*Journal of Waterway,Port, Coastal and Ocean Engineering*, ASCE, 133(6): 313-320.

9. Crespo, A.J.C., Dominguez, J.M., Gomez-Gesteira, M., Barreiro, A., and Rogers, B.D., (2012) “User Guide for DualSPHysics code.” DualSPHysics_v2.0.

10. *Gomez-Gesteira, M., Crespo, A.J.C., Rogers, B.D., Dalrymple, R.A., Dominguez, J.M. and Barreiro, A. (2012b) “SPHysics - development of a free-surface fluid solver- Part 2: Efficiency and test cases.” Computers & Geosciences, Elsevier,* 48: 300-307, *doi:10.1016/j.cageo.2012.02.028*.

11. Graf, W.H. and Istiarto, I. (2002) “Flow pattern in the scour hole around a cylinder.” *Journal of Hydraulic Research*, 40:13-20.
12. Groenenboom, P.H.L. and Cartwright, B.K. (2010) “Hydrodynamics and fluid- structure interaction by couples SPH-FE method.” *Journal of Hydraulic Research*, IAHR, 48: 61-73.
13. Hopton, S. (2010) “Modelling Open Channel Flow.” Thesis (PhD), University of Nottingham, UK.
14. Landers, M.N. and Mueller, D.S. (1996) “Channel scour at bridges in the United